The Geometry of the Universe

Hubert L. Bray
Duke University

University of Waterloo
Monday, March 9, 2015

The Geometry of the Universe

In a 1916 paper, Hilbert computed the Euler-Lagrange equation for the integral of the scalar curvature (plus other terms) over a manifold. The resulting equation connects quite beautifully to questions concerning geodesics, minimal surfaces, Ricci and scalar curvature, metric singularities, and geometric flows.

Amazingly, this equation, now known as the Einstein equation of general relativity, also replaced Newtonian physics as our current best description of the large-scale structure of the universe by explaining gravity and predicting gravitational lensing, black holes, the Big Bang, and quite arguably even the accelerating expansion of the universe - before they were observed. This raises a natural question: What other geometric ideas describe the universe?

The Puzzle of the Spirals

"Much as the discovery of these strange forms may be calculated to excite our curiosity, and to awaken an intense desire to learn something of the laws which give order to these wonderful systems, as yet, I think, we have no fair ground even for plausible conjecture."

Lord Rosse (1850)

The Puzzle of the Spirals

"Much as the discovery of these strange forms may be calculated to excite our curiosity, and to awaken an intense desire to learn something of the laws which give order to these wonderful systems, as yet, I think, we have no fair ground even for plausible conjecture."

Lord Rosse (1850)

"A beginning has been made by Jeans and other mathematicians on the dynamical problems involved in the structure of the spirals."

Curtis (1919)

The Puzzle of the Spirals

"Much as the discovery of these strange forms may be calculated to excite our curiosity, and to awaken an intense desire to learn something of the laws which give order to these wonderful systems, as yet, I think, we have no fair ground even for plausible conjecture."

Lord Rosse (1850)

"A beginning has been made by Jeans and other mathematicians on the dynamical problems involved in the structure of the spirals."

Curtis (1919)

"Incidentally, if you are looking for a good problem..."

Feynman (1963)

The Puzzle of the Spirals

"The old puzzle of the spiral arms of galaxies continues to taunt theorists. The more they manage to unravel it, the more obstinate seems the remaining dynamics. Right now, this sense of frustration seems greatest in just that part of the subject which advanced most impressively during the past decade - the idea of Lindblad and Lin that the grand bisymmetric spiral patterns, as in M51 and M81, are basically compression waves felt most intensely by the gas in the disks of those galaxies. Recent observations leave little doubt that such spiral "density waves" exist and indeed are fairly common, but no one still seems to know why.

To confound matters, not even the N-body experiments conducted on several large computers since the late 1960s have yet yielded any decently long-lived regular spirals."

Toomre (1977)

Big Questions

There is roughly five times more dark matter in the universe than regular baryonic matter represented by the periodic table.

Also, most of the mass of galaxies is dark matter.

1. What is the nature of dark matter?

2. Does dark matter have something to do with spiral structure in galaxies?

Spiral Galaxy M81

Spiral Galaxy M74

Spiral Galaxy NGC1365

Spiral Galaxy NGC4622

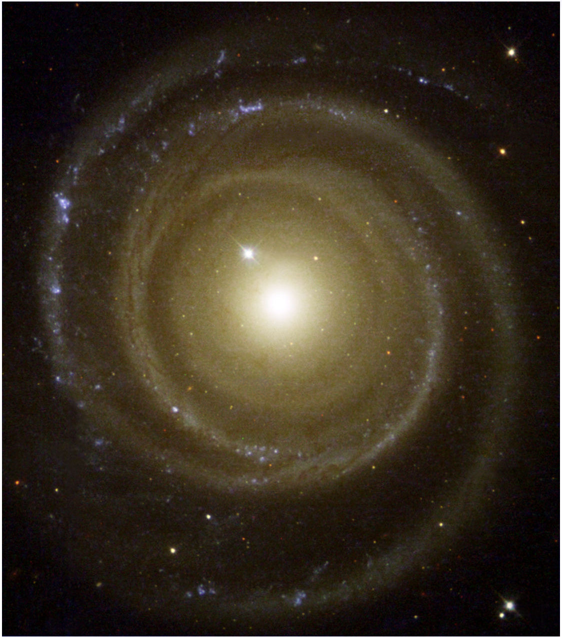

Spiral Galaxy M51, the Whirlpool Galaxy

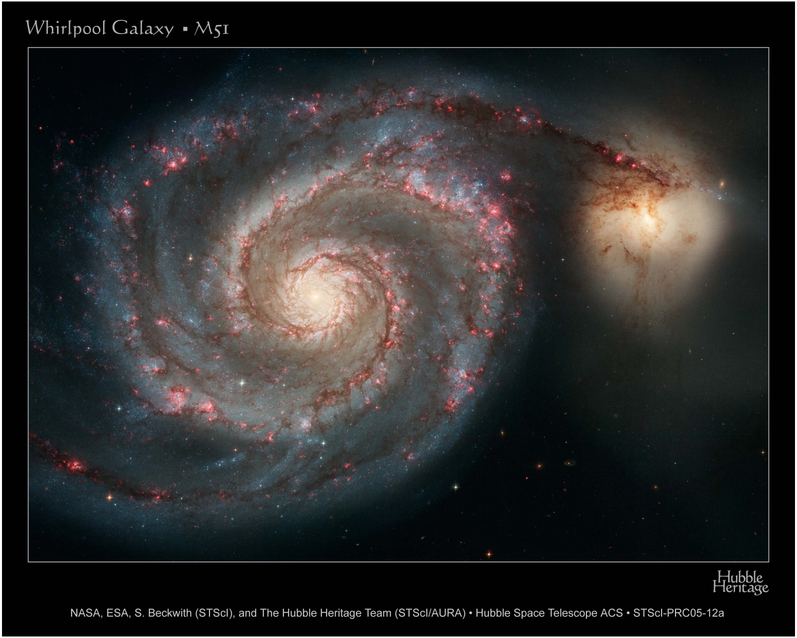

Spiral Galaxies 2MASX J00482185-2507365

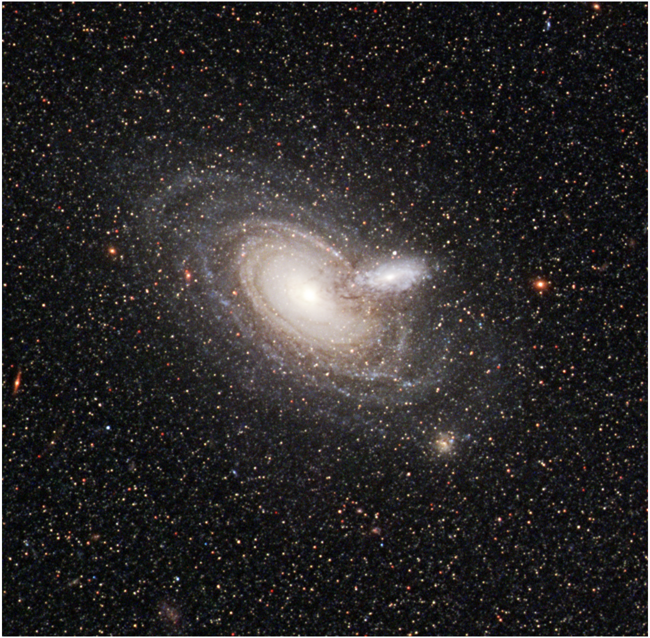

Spiral Galaxy NGC3314

Spiral Galaxies ARP274

Galaxy Cluster MS1054-0321

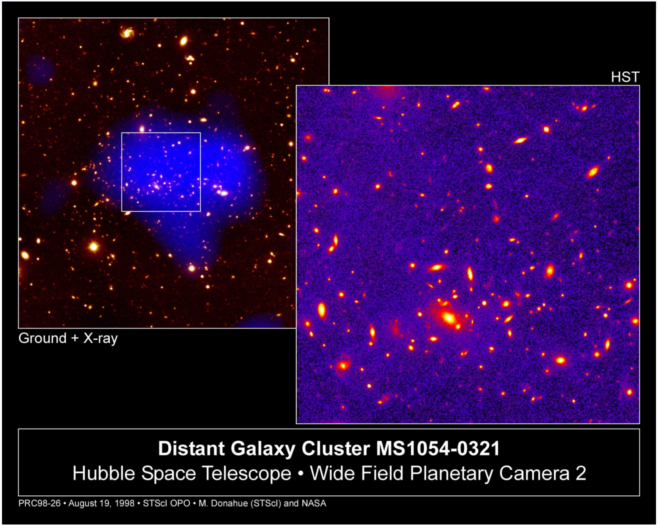

The mass of galaxy clusters is roughly 5% galaxies, 10% intergalactic gas, and 85% dark matter.

The Bullet Cluster

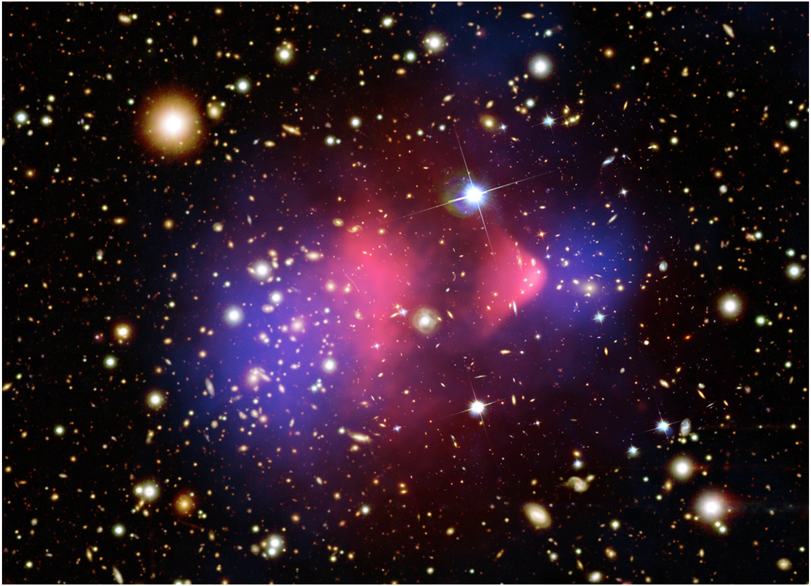

SPIRALS

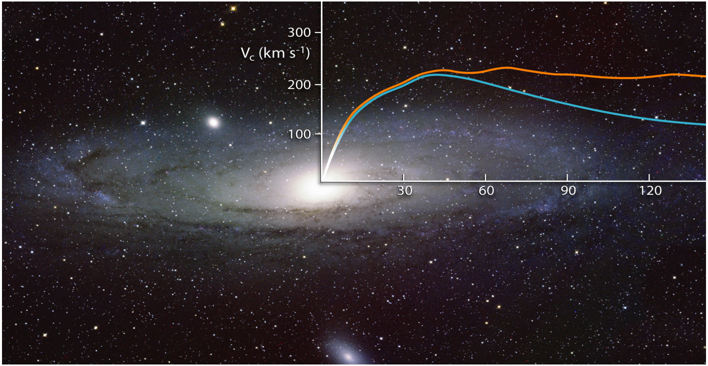

Figure : From the Dark Matter Awareness Week presentation. Presentation review at arXiv:1102.1184v1 by Paolo Salucci, Christiane Frigerio Martins, and Andrea Lapi.

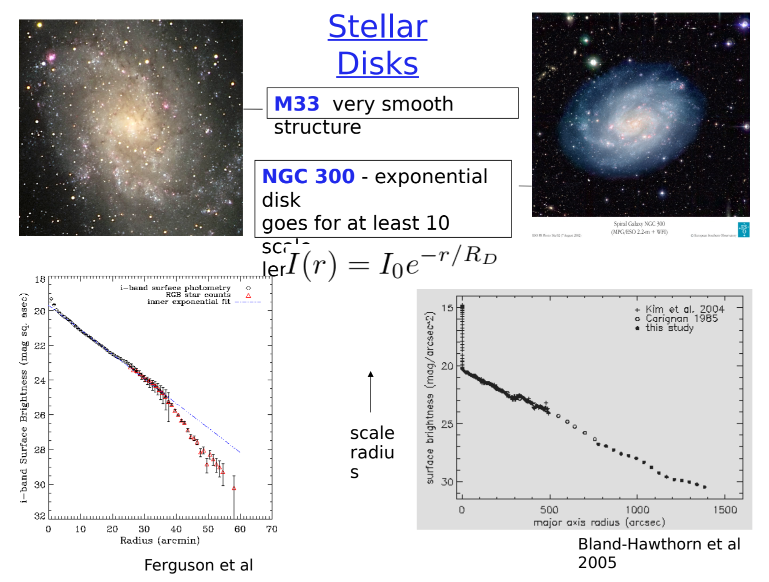

Figure : From the Dark Matter Awareness Week presentation. Presentation review at arXiv:1102.1184v1 by Paolo Salucci, Christiane Frigerio Martins, and Andrea Lapi.

The distribution of DM around spirals

Using individual galaxies Gentile+ 2004, de Blok+ 2008 Kuzio de Naray+ 2008, Oh+ 2008, Spano+ 2008, Trachternach+ 2008, Donato+,2009

A detailed investigation: high quality data and model independent analysis

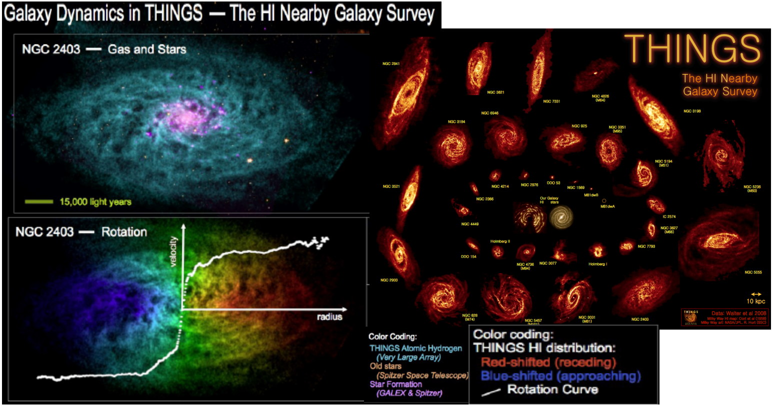

Figure : From the Dark Matter Awareness Week presentation. Presentation review at arXiv:1102.1184v1 by Paolo Salucci, Christiane Frigerio Martins, and Andrea Lapi.

Early discovery from optical and HI RCs

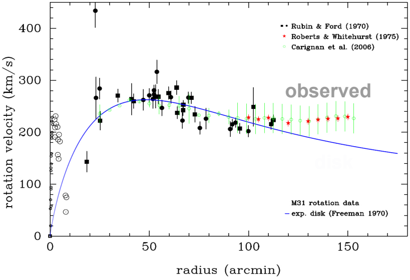

no RC follows the disk velocity profile

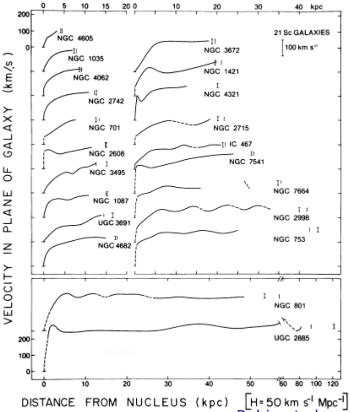

Rubin et al 1980

Mass discrepancy AT OUTER RADII

Figure : From the Dark Matter Awareness Week presentation. Presentation review at arXiv:1102.1184v1 by Paolo Salucci, Christiane Frigerio Martins, and Andrea Lapi.

Rotation Curves

TYPICAL INDIVIDUAL RCs OF INCREASING LUMINOSITY

Coadded from 3200 individual RC

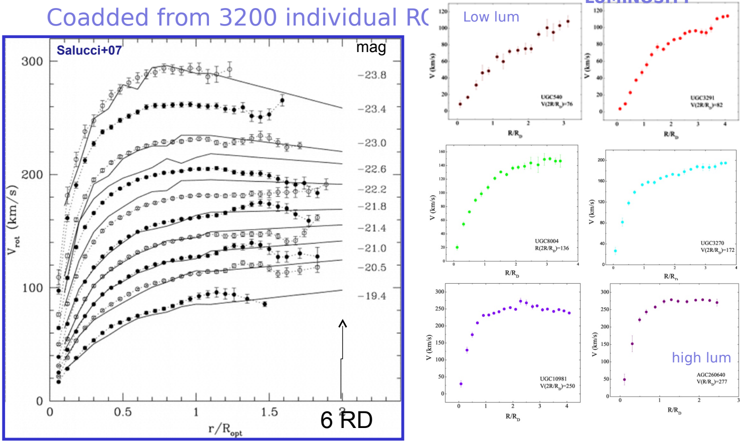

Figure : From the Dark Matter Awareness Week presentation. Presentation review at arXiv:1102.1184v1 by Paolo Salucci, Christiane Frigerio Martins, and Andrea Lapi.

The Mass of the Universe

70% **Dark Energy**
(the cosmological constant of **General Relativity** used to explain the observed *accelerating* expansion of the universe)

25% **Dark Matter**

5% **Regular Baryonic Matter**
(Gas, Dust, Planets, Stars, etc., composed of particles described by **Quantum Field Theory and the Standard Model of Particle Physics**)

Which theory best describes Dark Matter?

Successes of General Relativity: The Big Bang

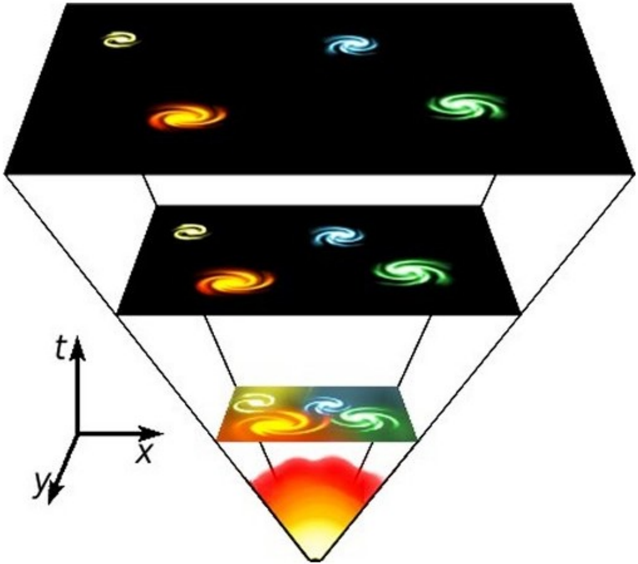

Successes of General Relativity: The *Accelerating* Expansion of the Universe

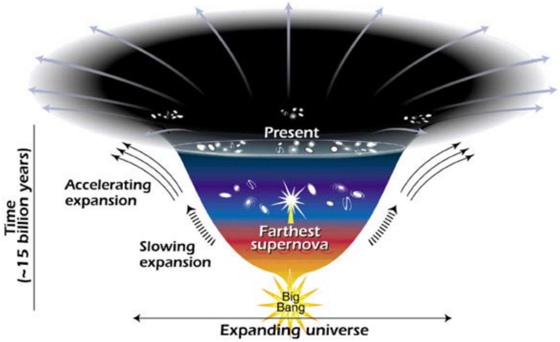

Based on papers in 1998 and 1999, the 2011 Nobel Prize in Physics was awarded to Perlmutter, Schmidt, and Riess "for the discovery of the accelerating expansion of the Universe through observations of distant supernovae."

Successes of General Relativity: Black Holes

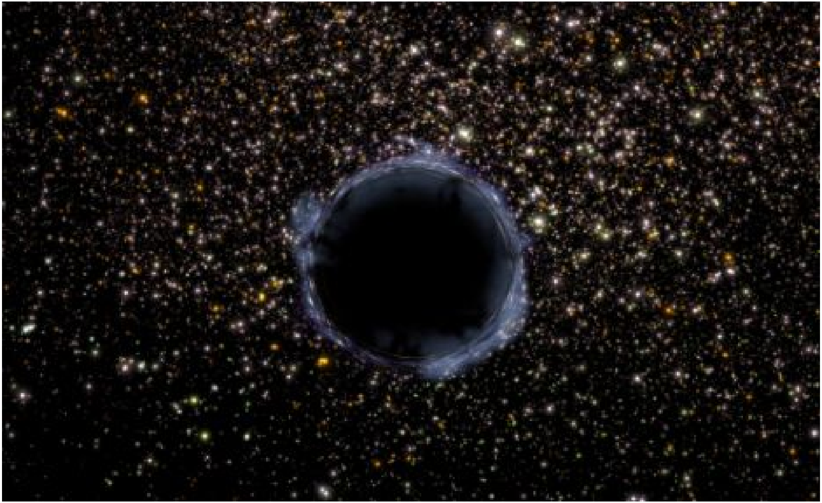

Artist's rendition of a black hole.

Successes of General Relativity: Black Holes

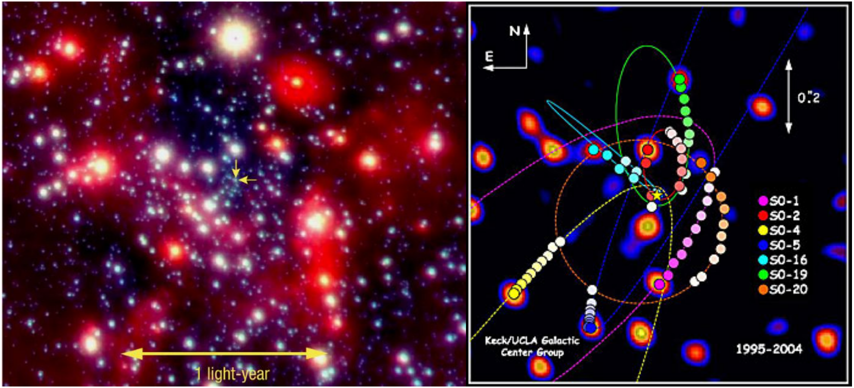

The supermassive black hole (4 million solar masses) at the center of the Milky Way Galaxy.

Successes of General Relativity: Gravity

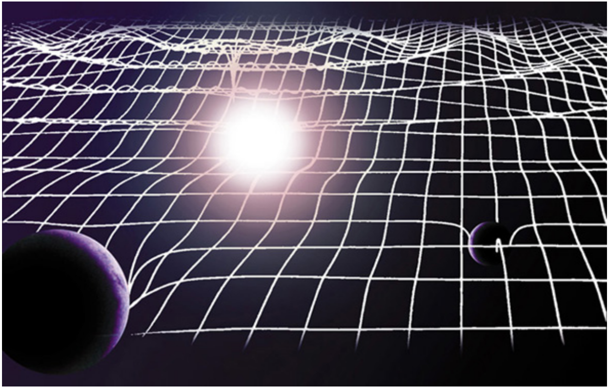

The Earth goes around the Sun because the mass of the Sun curves spacetime, not because of some mysterious $1/r^2$ force law assumed as an axiom without any explanation as to what the mechanism for gravity might be.

Successes of General Relativity: Gravitational Lensing

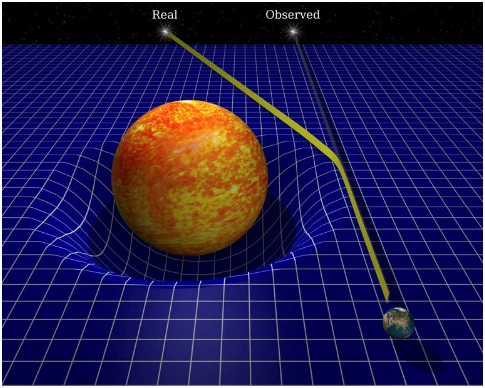

General Relativity agrees with observations and predicts *twice* the bending angle for light that Newtonian physics predicts.

What about Dark Matter and Spiral Galaxies?

Idea 1: Natural geometric axioms motivate studying the Einstein-Klein-Gordon equations with a cosmological constant. Is the scalar field of the Klein-Gordon equation dark matter?

Idea 2: Wave types of equations, such as the Klein-Gordon equation, naturally form density waves in their matter densities.

Idea 3: Density waves in dark matter, through gravity, naturally form density waves in the regular baryonic matter. Does this explain the observed spiral density waves in spiral galaxies?

Spiral Galaxy Simulation #1

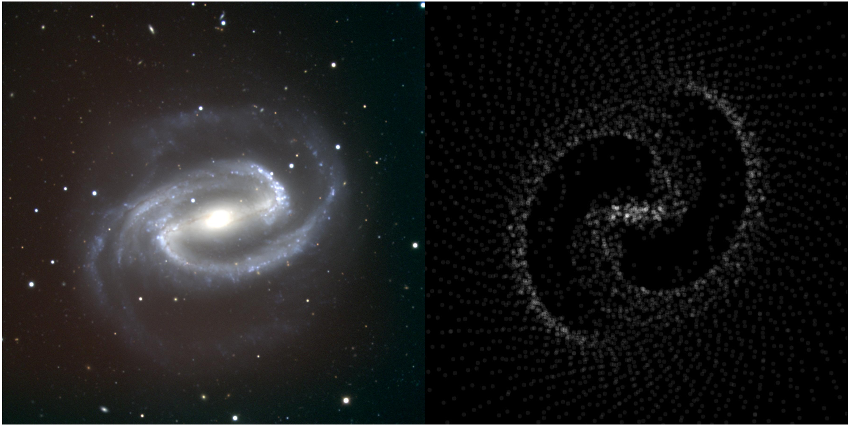

NGC1300 on the left, simulation on the right.

Spiral Galaxy Simulation #2

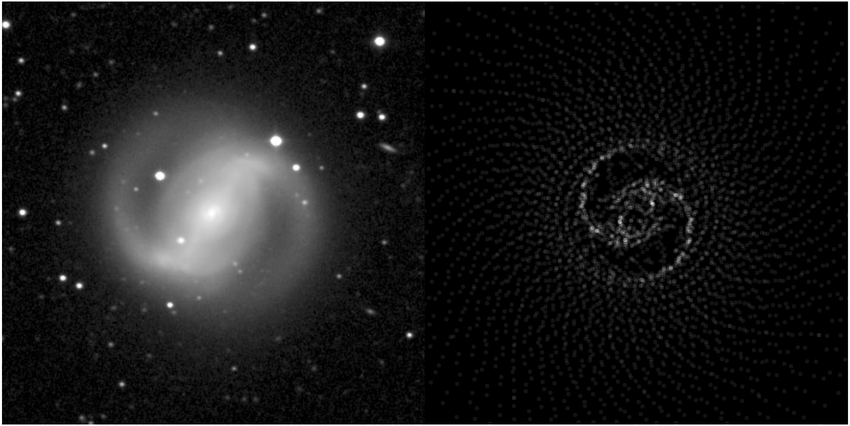

NGC4314 on the left, simulation on the right.

Spiral Galaxy Simulation #3

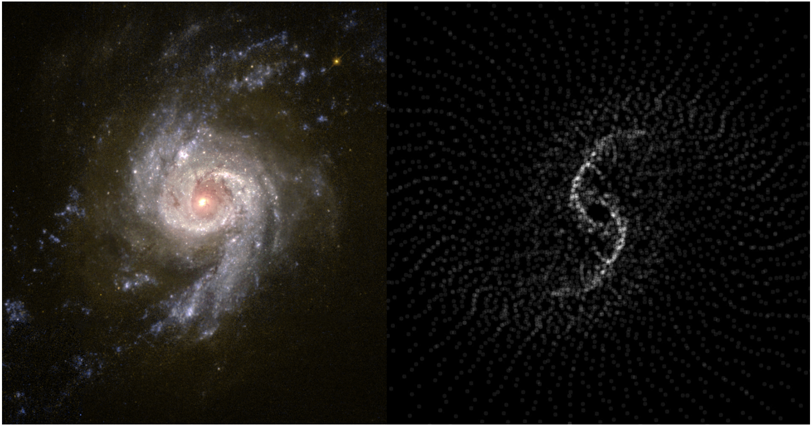

NGC3310 on the left, simulation on the right.

Spiral Galaxy Simulation #4

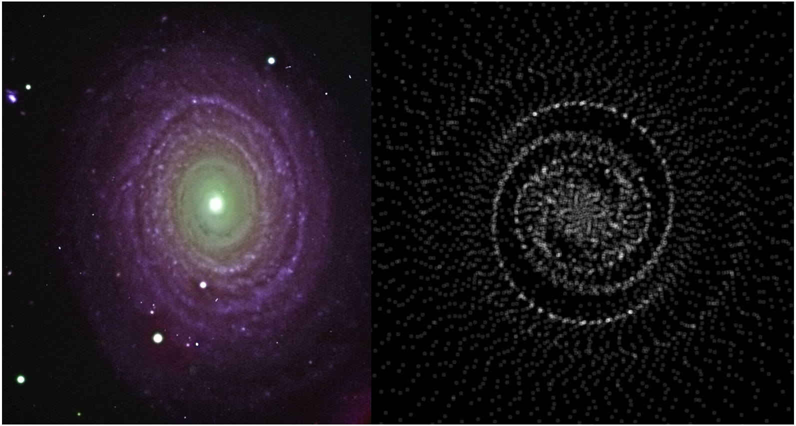

NGC488 on the left, simulation on the right.

Philosophy

General Relativity results from Special Relativity when the assumption that the spacetime metric is the standard flat one is *removed*.

The assumption that the metric is flat is replaced by the axiom that the spacetime metric is a critical point of an action functional. By Noether's theorem, spacetimes which are critical points of action functionals have conserved quantities, one for each symmetry of the action, which is great since conserved quantities like energy and momentum are fundamental observations.

Natural question:

What theory results when the assumption that the connection on the spacetime is the standard Levi-Civita one is removed? What should the action be? Even more fundamentally, what properties should the action have?

Philosophy

Axiom 0

The universe is described by a smooth manifold N *which is Hausdorff and second countable with smooth metric* g *of signature* $(- + ++)$ *at every point and a smooth connection* ∇*.*

A smooth manifold N is a Hausdorff space with a complete atlas of smoothly overlapping coordinate charts. Hence, we see that coordinate charts are more than convenient places to do calculations, but are in fact a necessary part of the definition of a smooth manifold.

Philosophy

Given a fixed coordinate chart, let $\{\partial_i\}$, $0 \le i \le 3$, be the tangent vector fields to N corresponding to the standard basis vector fields of the coordinate chart.

Let $g_{ij} = g(\partial_i, \partial_j)$ and $\Gamma_{ijk} = g(\nabla_{\partial_i}\partial_j, \partial_k)$, and let

$$M = \{g_{ij}\} \quad , \quad C = \{\Gamma_{ijk}\} \quad , \quad M' = \{g_{ij,k}\} \quad \text{and} \quad C' = \{\Gamma_{ijk,l}\}$$

be the components of the metric and the connection in the coordinate chart and all of the first derivatives of these components in the coordinate chart.

Philosophy

Axiom 1

For all coordinate charts $\Phi : \Omega \subset N \to R^4$ *and open sets* U *whose closure is compact and in the interior of* Ω, (g, ∇) *is a critical point of the functional*

$$F_{\Phi,U}(g,\nabla) = \int_{\Phi(U)} \mathit{Quad}_M(M' \cup M \cup C' \cup C)\, dV_{R^4}$$

with respect to smooth variations of the metric and connection compactly supported in U, *for some fixed quadratic functional* $Quad_M$ *with coefficients in* M, *where we define*

$$\mathit{Quad}_Y(\{x_\alpha\}) = \sum_{\alpha,\beta} F^{\alpha\beta}(Y) x_\alpha x_\beta$$

for some fixed functions $\{F^{\alpha\beta}\}$.

Philosophy

Note that we have not arbitrarily specified the action, only the form of the action. Also note that while there is one action for each coordinate chart, (g, ∇) must be a critical point of these actions in *all* coordinate charts and hence does not depend on any one particular coordinate chart.

$\text{Quad}_M(M') \longrightarrow$ Vacuum Einstein Equation

$\text{Quad}_M(M' \cup M) \longrightarrow$ Vacuum Einstein Equation with a Cosmological Constant

$\text{Quad}_M(M' \cup M \cup C' \cup C) \longrightarrow$ Einstein-Klein-Gordon Equations with a Cosmological Constant

When the integrand in Axiom 1 is replaced with the above expressions, we get the corresponding three systems of equations on the right. The first two statements follow from the works of Cartan, Weyl, Vermeil, and Lovelock. The last statement is what we will now discuss.

The Einstein-Hilbert Action

Standard calculations show that the formula for the scalar curvature in terms of the metric in a coordinate chart is

$$
\begin{aligned}
R &= (g^{ik}g^{jl} - g^{ij}g^{kl})\underline{g_{ij,kl}} + \underline{g_{ij,k}g_{ab,c}} \cdot \\
&\quad \left(\frac{3}{4}g^{ia}g^{jb}g^{kc} - \frac{1}{2}g^{ia}g^{jc}g^{kb} - g^{ia}g^{jk}g^{bc} - \frac{1}{4}g^{ij}g^{ab}g^{kc} + g^{ij}g^{ac}g^{kb}\right)
\end{aligned}
$$

Then since $dV = |g|^{1/2}\, dV_{R^4}$, integrating by parts gives

$$
\begin{aligned}
\int_U R\, dV &= \text{boundary term} + \int_{\Phi(U)} \underline{g_{ij,k}g_{ab,c}} \cdot |g|^{1/2}\, dV_{R^4} \cdot \\
&\quad \left(-\frac{1}{4}g^{ia}g^{jb}g^{kc} + \frac{1}{2}g^{ia}g^{jc}g^{kb} + \frac{1}{4}g^{ij}g^{ab}g^{kc} - \frac{1}{2}g^{ij}g^{ac}g^{kb}\right)
\end{aligned}
$$

The Einstein-Hilbert action fits the form of Axiom 1 with no connection terms. This is why the resulting Euler-Lagrange equation, $G = 0$, is second order in the metric.

The General Form of a Connection

By the Koszul formula, the standard Levi-Civita connection has components

$$\bar{\Gamma}_{ijk} = \frac{1}{2}\left(g_{ik,j} + g_{jk,i} - g_{ij,k}\right),$$

The difference of two connections is a tensor, so let

$$D_{ijk} = \Gamma_{ijk} - \bar{\Gamma}_{ijk}.$$

Define

$$\begin{aligned} T_{ijk} &= D_{ijk} - D_{jik} \\ &= (\Gamma_{ijk} - \bar{\Gamma}_{ijk}) - (\Gamma_{jik} - \bar{\Gamma}_{jik}) \\ &= \Gamma_{ijk} - \Gamma_{jik} \end{aligned}$$

which we recognize as the components of the torsion tensor. Note that T_{ijk}, unlike D_{ijk}, does *not* depend on derivatives of the metric.

Define

$$\begin{aligned}\gamma_{ijk} &= \frac{1}{6}(T_{ijk} + T_{jki} + T_{kij}) \\ &= \frac{1}{6}(D_{ijk} - D_{jik} + D_{jki} - D_{kji} + D_{kij} - D_{ikj}) \\ &= \frac{1}{6}(\Gamma_{ijk} - \Gamma_{jik} + \Gamma_{jki} - \Gamma_{kji} + \Gamma_{kij} - \Gamma_{ikj})\end{aligned}$$

to be the fully antisymmetric part of the difference tensor D. Thus, γ_{ijk} are the components of a three form. Hence,

$$d\gamma_{ijkl} = \gamma_{jkl,i} - \gamma_{kli,j} + \gamma_{lij,k} - \gamma_{ijk,l}$$

are the antisymmetric coefficients of the tensor $d\gamma$ which do *not* involve derivatives of the metric, just derivatives of Γ. Hence, functionals of the form

$$F_{\Phi,U}(g,\nabla) = \int_U (cR - 2\Lambda - \frac{c_3}{24}|d\gamma|^2 - \mathsf{Quad}_g(D))\, dV,$$

are allowed by Axiom 1, up to a boundary term which is irrelevant for the Euler-Lagrange equations produced. Conjecture: this is it.

The Action

In the simplest representative case, we can choose $D_{ijk} = \gamma_{ijk}$ with action functional

$$\begin{aligned} F_{\Phi,U}(g,\nabla) &= \int_U (R - 2\Lambda - \frac{c_3}{24}|d\gamma|^2 - \frac{c_4}{6}|\gamma|^2)\, dV \\ &= \int_U (R - 2\Lambda - c_3|d\gamma|^2_{4-form} - c_4|\gamma|^2_{3-form})\, dV \end{aligned}$$

Equivalently, if we let

$$\gamma = *(v^*),$$

where v is a vector field, v^* is the 1 form dual to v, and $*$ is the Hodge star operator, then the action becomes

$$F_{\Phi,U}(g,\nabla) = \int_U (R - 2\Lambda + c_3(\nabla \cdot v)^2 + c_4|v|^2)\, dV,$$

where $\nabla \cdot v$ denotes the divergence of v.

The Euler-Lagrange equations for this action are

$$\begin{aligned} G + \Lambda g &= c_4\, v^* \otimes v^* - \frac{1}{2}\left(c_3(\nabla \cdot v)^2 + c_4|v|^2\right) g \\ \nabla(\nabla \cdot v) &= \frac{c_4}{c_3} v. \end{aligned}$$

For the dominant energy condition to be satisfied, we need $c_3, c_4 \geq 0$. To arrive at a nontrivial equation for v we need $c_3 \neq 0$ and to arrive at a deterministic equation for v we need $c_4 \neq 0$. Hence, let's take $c_3, c_4 > 0$. Now let

$$f = \left(\frac{c_3}{c_4}\right)^{1/2} \nabla \cdot v \qquad \Rightarrow \qquad v = \left(\frac{c_3}{c_4}\right)^{1/2} \nabla f$$

and

$$\begin{aligned} G + \Lambda g &= c_3\, \left\{ df \otimes df - \frac{1}{2}\left(|df|^2 + \frac{c_4}{c_3} f^2\right) g \right\} \\ \Box_g f &= \frac{c_4}{c_3} f \end{aligned}$$

which has a solution if and only if the original system does.

The Einstein-Klein-Gordon Equations

$$\begin{aligned} G + \Lambda g &= 8\pi\mu_0 \left\{ 2\frac{df \otimes df}{\Upsilon^2} - \left(\frac{|df|^2}{\Upsilon^2} + f^2 \right) g \right\} \\ \Box_g f &= \Upsilon^2 f \end{aligned}$$

where G is the Einstein curvature tensor, f is the scalar field representing dark matter, Λ is the cosmological constant, and Υ is a new fundamental constant of nature whose value has yet to be determined. Note that the connection will have components

$$\Gamma_{ijk} = \frac{1}{\Upsilon}(*df)_{ijk} + \frac{1}{2}\left(g_{ik,j} + g_{jk,i} - g_{ij,k}\right).$$

Deep question: The effect of the connection is seen gravitationally as the scalar field f, but does the connection manifest itself physically in any other way?

Wave Dark Matter is Automatically Cold

Suppose that the spacetime metric is both homogeneous and isotropic, and hence is the Friedmann-Lemaître-Robertson-Walker metric $-dt^2 + a(t)^2 ds_\kappa^2$, where ds_κ^2 is the constant curvature metric of curvature κ. Then f is solely a function of t.

Furthermore, if we let $H(t) = a'(t)/a(t)$ be the Hubble constant, and $\bar{\rho}$ and $\bar{P}$ be the average energy density and average pressure of the scalar field for $a \leq t \leq b$, then

$$\frac{\bar{P}}{\bar{\rho}} = \frac{\epsilon}{1+\epsilon} \qquad \text{where} \qquad \epsilon = -\frac{3\overline{H'}}{4\Upsilon^2}$$

and

$$\overline{H'} = \frac{\int_a^b H'(t) f(t)^2 \, dt}{\int_a^b f(t)^2 \, dt},$$

where a, b are two zeros of f (for example, two consecutive zeros).

$|H'(t)| \approx (10^{10} \text{ light years})^{-2}$. Could the average temperature of dark matter in the universe be used to estimate the value of Υ?

Solutions to the Klein-Gordon Equation on Static Spherically Symmetric Spacetimes

Suppose the spacetime metric has the form

$$ds^2 = -V(r)^2 dt^2 + V(r)^{-2} \left(dx^2 + dy^2 + dz^2 \right)$$

The function $V(r)$ acts likes the gravitational potential function from Newtonian physics but goes to one at infinity.

Then

$$f = A \cos(\omega t) \cdot Y_n(\theta, \phi) \cdot r^n \cdot f_{\omega,n}(r)$$

is a solution to the Klein-Gordon equation of this spacetime when

$$V(r)^2 \left(f''_{\omega,n}(r) + \frac{2(n+1)}{r} f'_{\omega,n}(r) \right) = \left(\Upsilon^2 - \frac{\omega^2}{V(r)^2} \right) f_{\omega,n}.$$

Rotating Wave Dark Matter Solutions

The solutions on which our simulations are based are of the form

$$f = A_0 \cos(\omega_0 t) f_{\omega_0,0}(r) + A_2 \cos(\omega_2 t - 2\phi) \sin^2(\theta) r^2 f_{\omega_2,2}(r).$$

Note that both $\cos(2\phi)\sin^2(\theta)$ and $\sin(2\phi)\sin^2(\theta)$ are second degree spherical harmonics, so this fits the previous form.

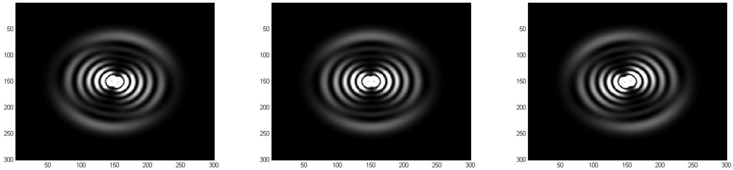

Figure : Exact solution to the Klein-Gordon equation in a fixed spherically symmetric potential well based on the Milky Way Galaxy at $t = 0$, $t = 10$ million years, and $t = 20$ million years. The pictures show the dark matter density (in white) in the xy plane. This solution, which one can see is rotating, has angular momentum.

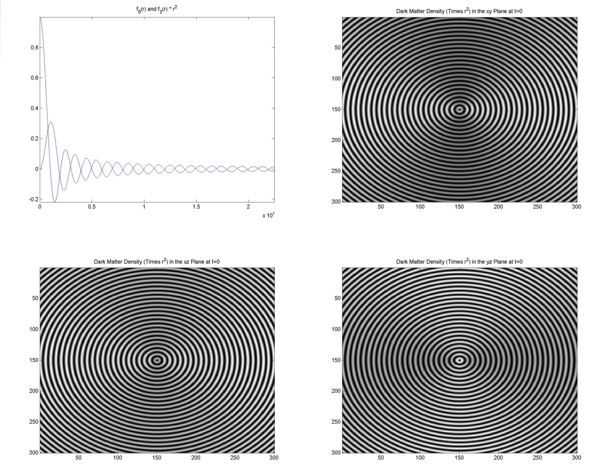

Figure : Spiral Galaxy Simulation # 2: Graphs of $f_{\omega_0,0}(r)$ and $r^2 f_{\omega_2,2}(r)$ for r up to $22,500$ light years (top left). The other three images, each with a radius of $22,500$ light years, are plots of the dark matter density (in white) times r^2 in the xy plane (top right), in the xz plane (bottom left), and in the yz plane (bottom right).

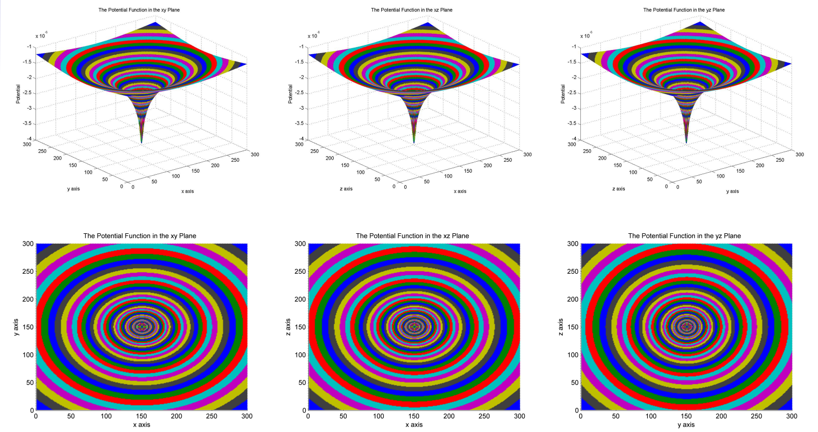

Figure : Graphs of the potential function in the xy plane (first column), the xz plane (second column), and the yz plane (third column) out to a radius of $22,500$ light years for Spiral Galaxy Simulation #2. The second row is the same as the first row except that the point of view is looking straight down so that we can see the level sets of the potential function in each plane. Note that the level sets are slightly ellipsoidal.

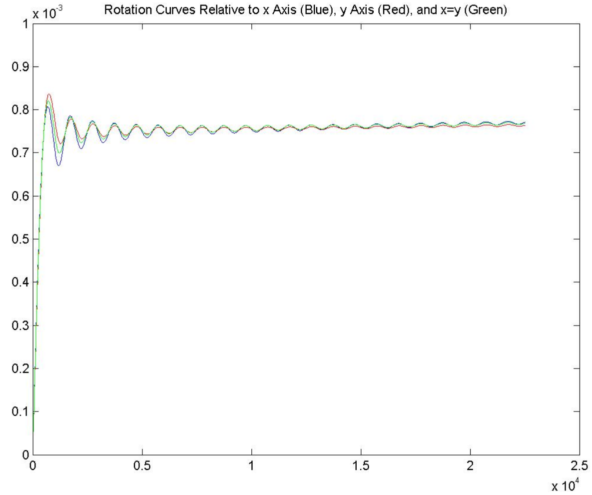

Figure : Approximate rotation curves for Spiral Galaxy Simulation #2. We have approximated the rotation curves with graphs of $\sqrt{r|\nabla V|}$ (which is exactly correct in the spherically symmetric case) along the x axis (in blue), along the y axis (in red), and along $y = x$ (in green).

Spiral Galaxy Simulation #2

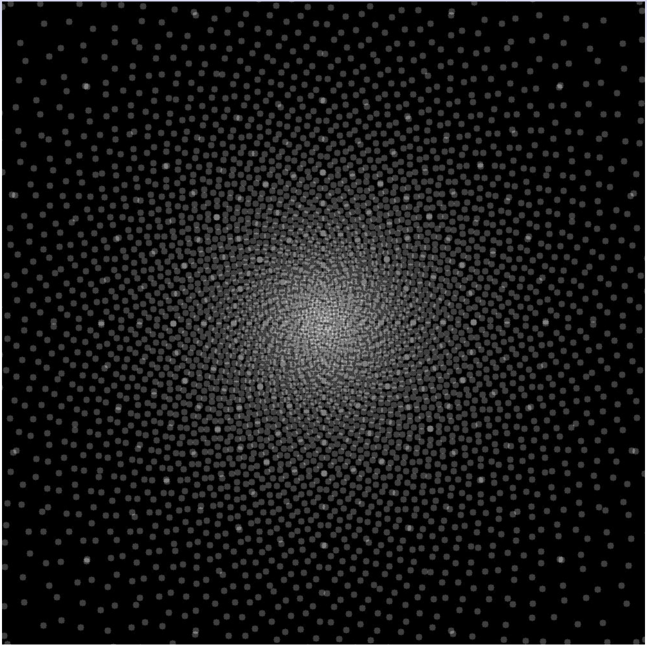

Figure : $t = 0$ million years for Spiral Galaxy Simulation #2.

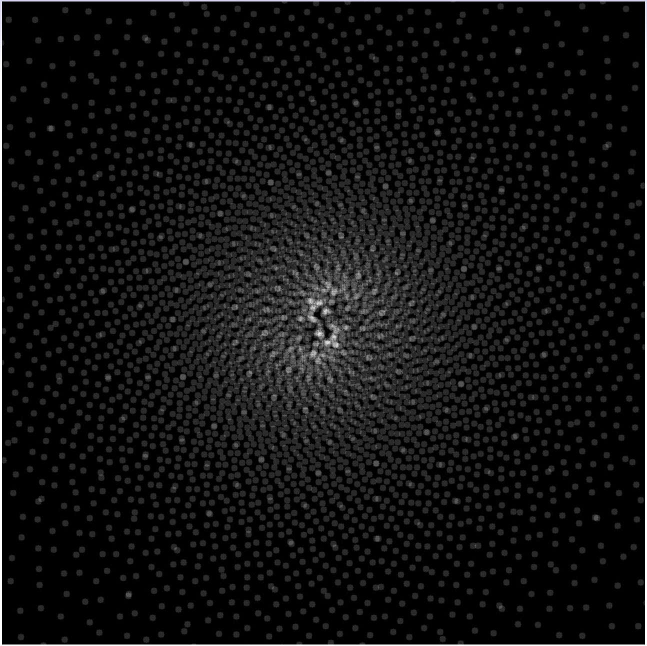

Figure : $t = 5$ million years for Spiral Galaxy Simulation #2.

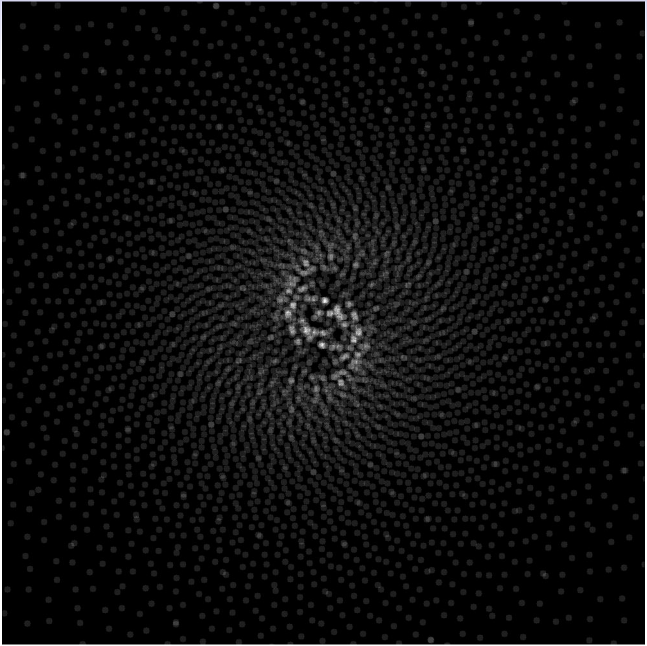

Figure : $t = 10$ million years for Spiral Galaxy Simulation #2.

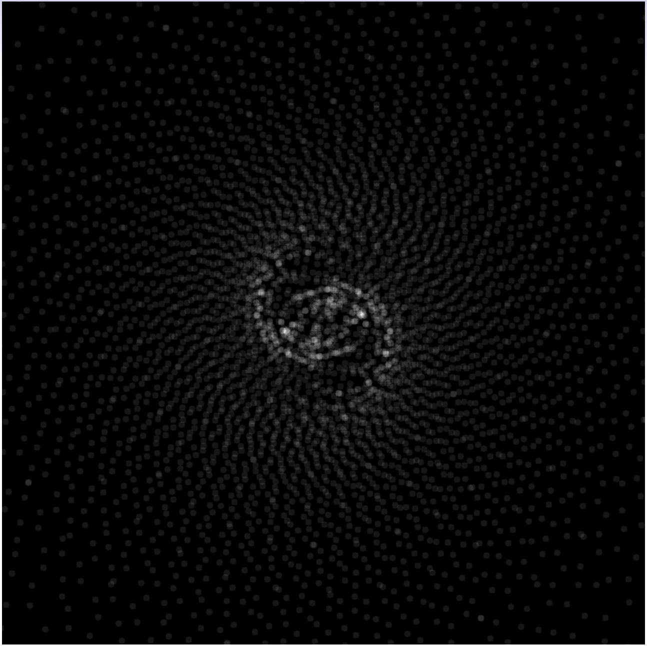

Figure : $t = 15$ million years for Spiral Galaxy Simulation #2.

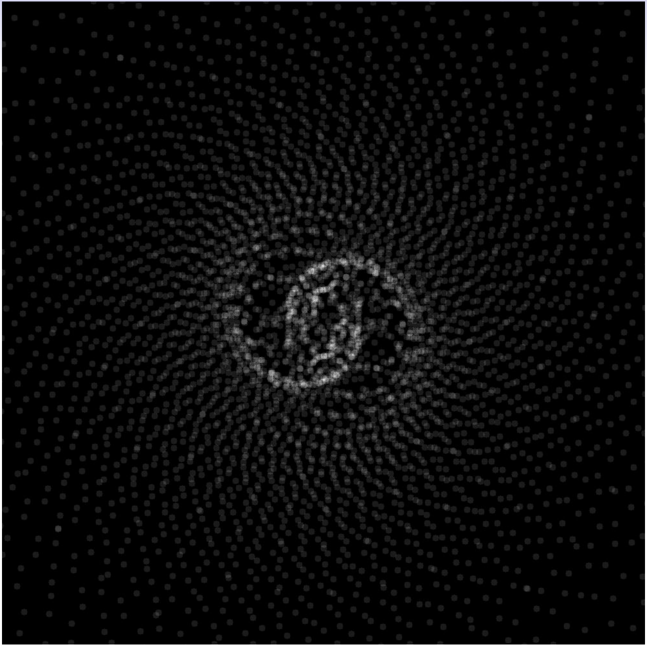

Figure : $t = 20$ million years for Spiral Galaxy Simulation #2.

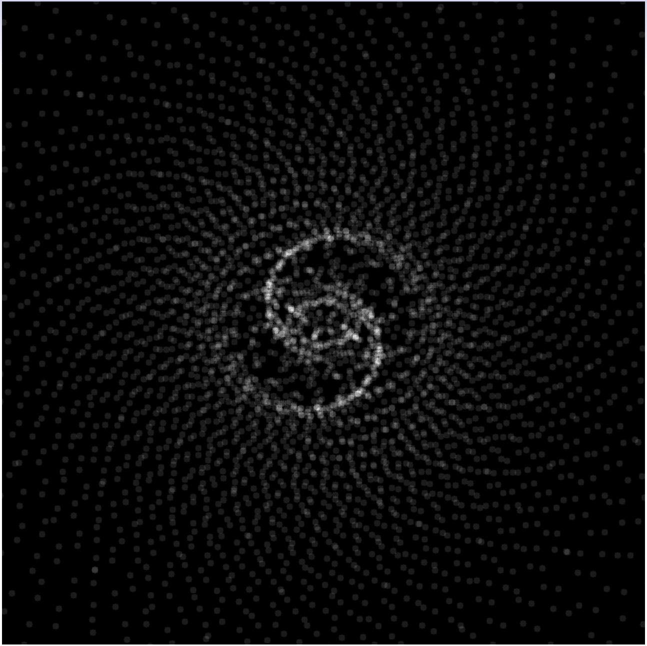

Figure : $t = 25$ million years for Spiral Galaxy Simulation #2.

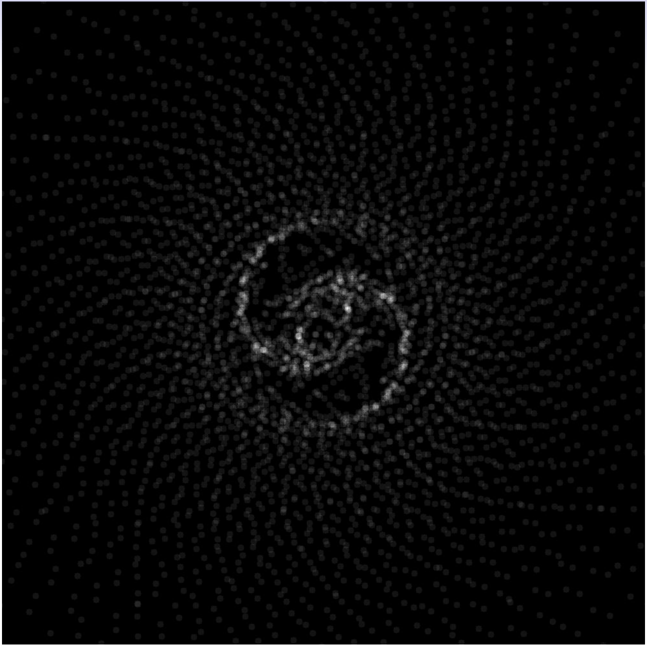

Figure : $t = 30$ million years for Spiral Galaxy Simulation #2.

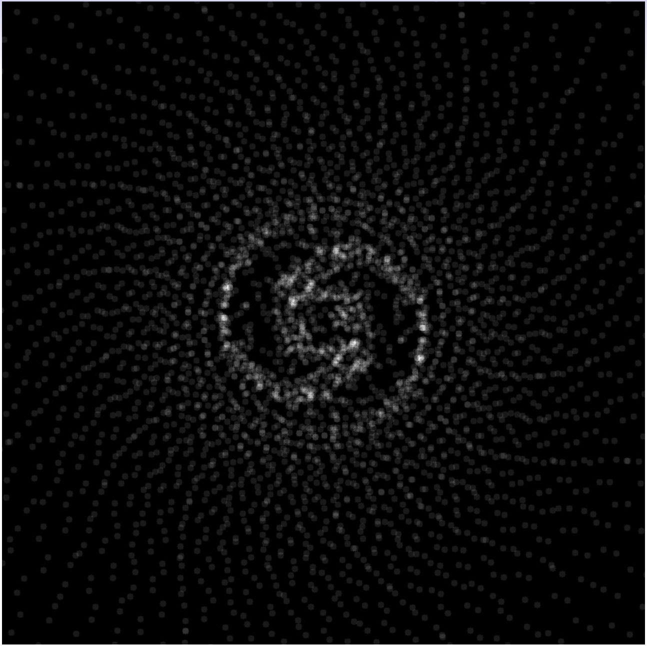

Figure : $t = 35$ million years for Spiral Galaxy Simulation #2.

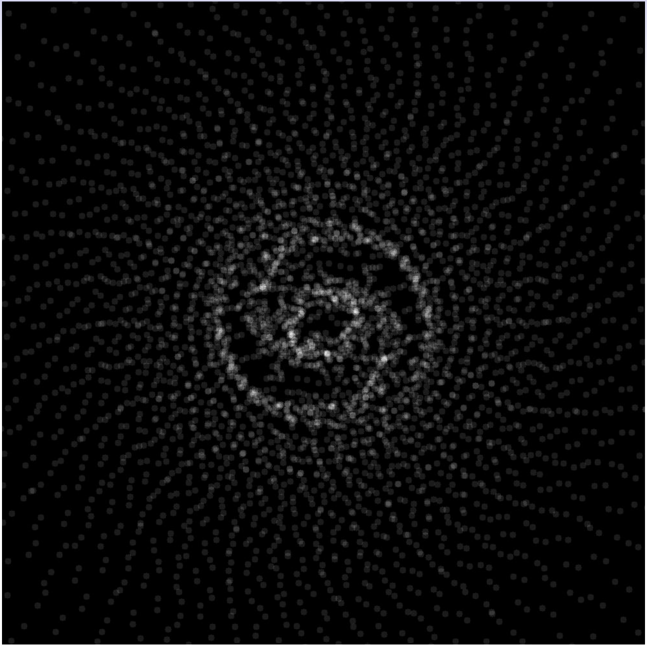

Figure : $t = 40$ million years for Spiral Galaxy Simulation #2.

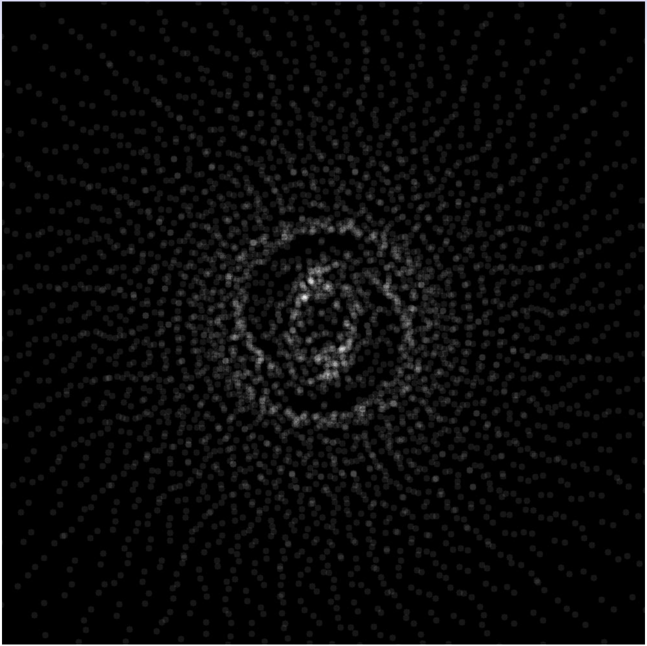

Figure : $t = 45$ million years for Spiral Galaxy Simulation #2.

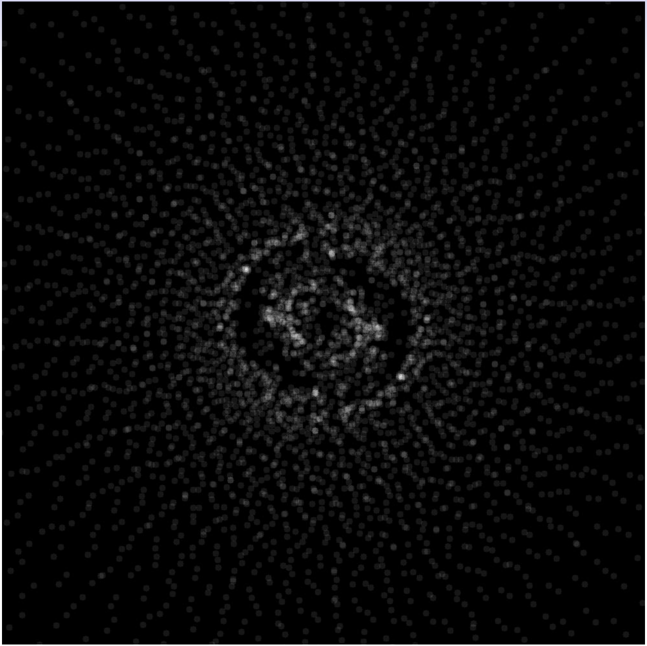

Figure : $t = 50$ million years for Spiral Galaxy Simulation #2.

Spiral Galaxy Simulation #2

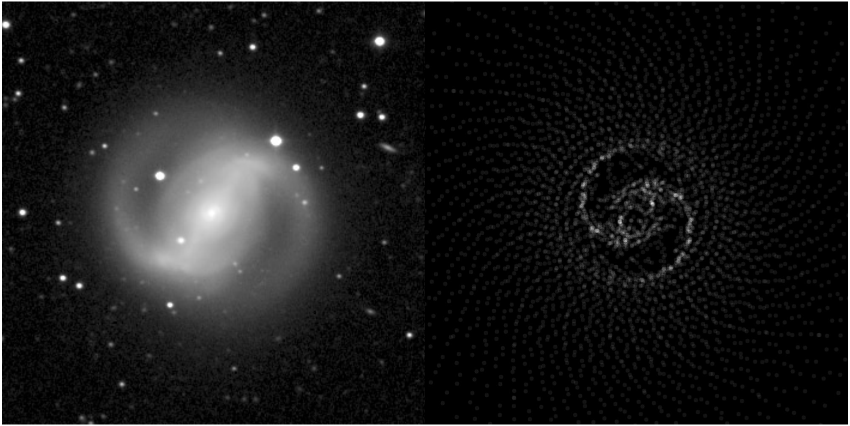

NGC4314 on the left, simulation on the right.

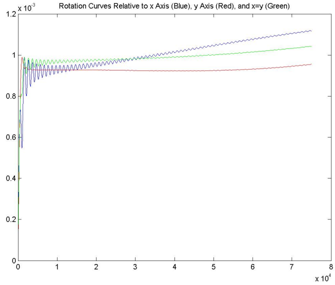

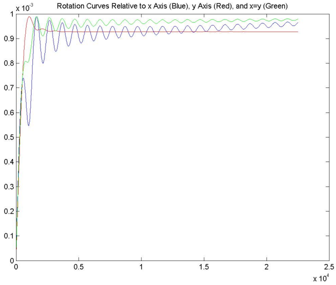

Figure : Approximate rotation curves for Spiral Galaxy Simulation $\#1$ out to a radius of $75,000$ light years (left) and $22,500$ light years (right). We have approximated the rotation curves with graphs of $\sqrt{r|\nabla V|}$ (which is exactly correct in the spherically symmetric case) along the x axis (in blue), along the y axis (in red), and along $y = x$ (in green).

Spiral Galaxy Simulation #1

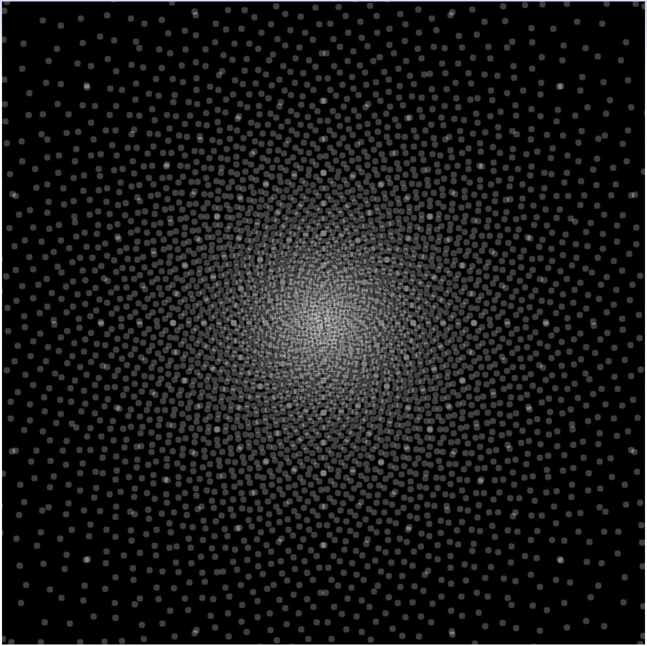

Figure : $t = 0$ million years for Spiral Galaxy Simulation #1.

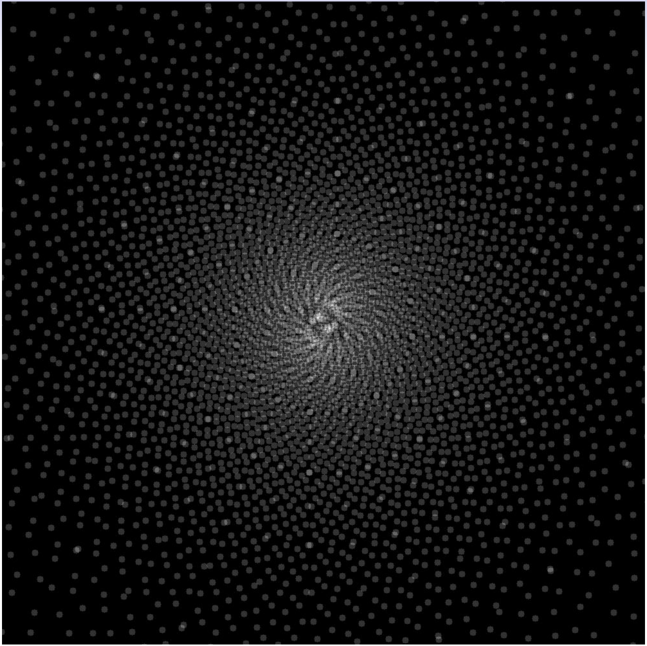

Figure : $t = 1$ million years for Spiral Galaxy Simulation #1.

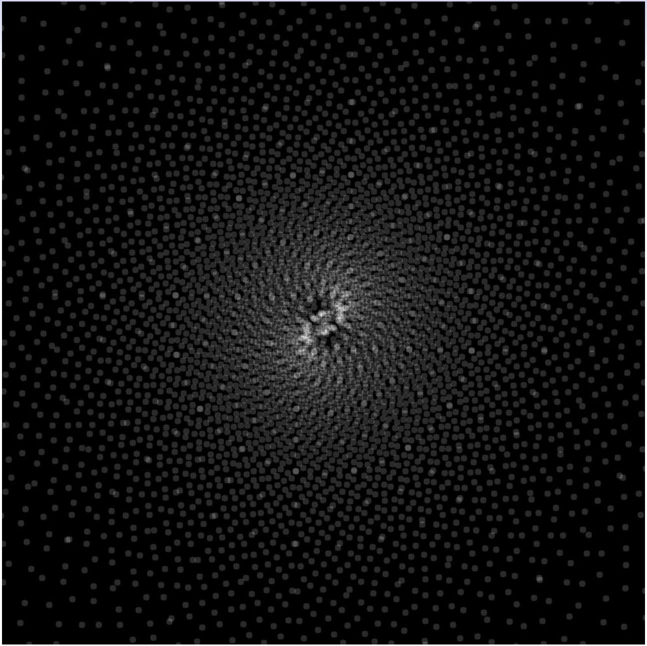

Figure : $t = 2$ million years for Spiral Galaxy Simulation #1.

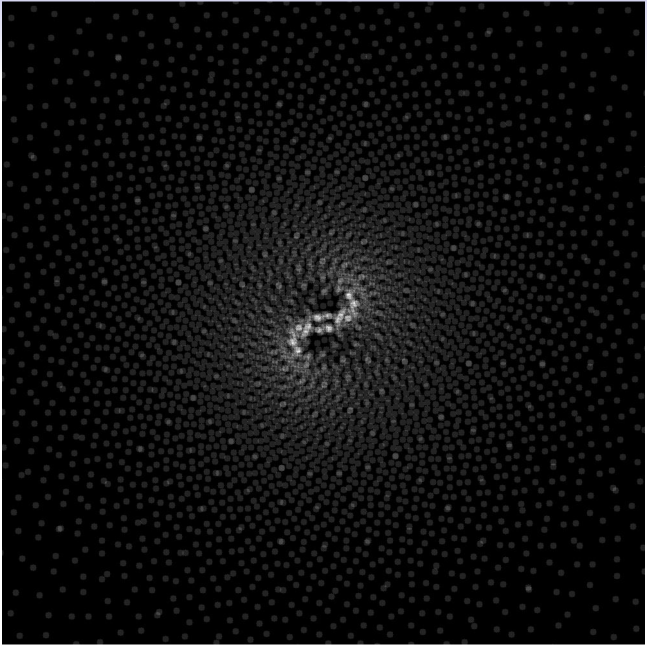

Figure : $t = 3$ million years for Spiral Galaxy Simulation #1.

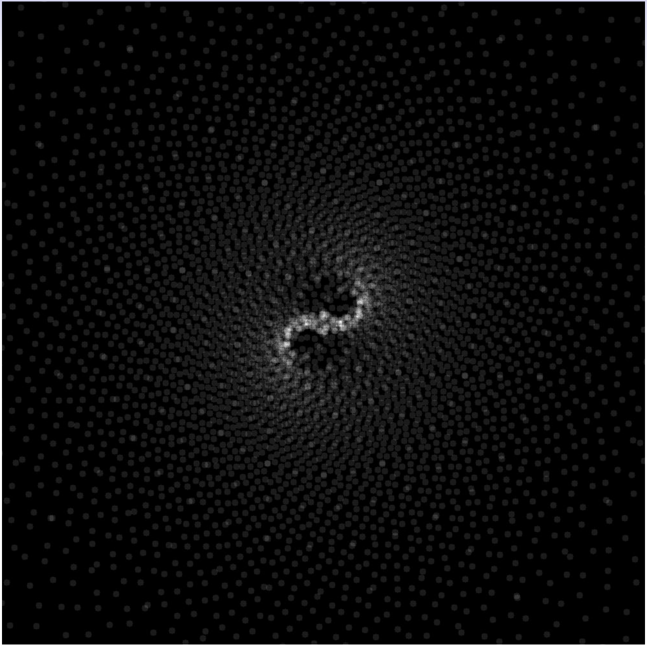

Figure : $t = 4$ million years for Spiral Galaxy Simulation #1.

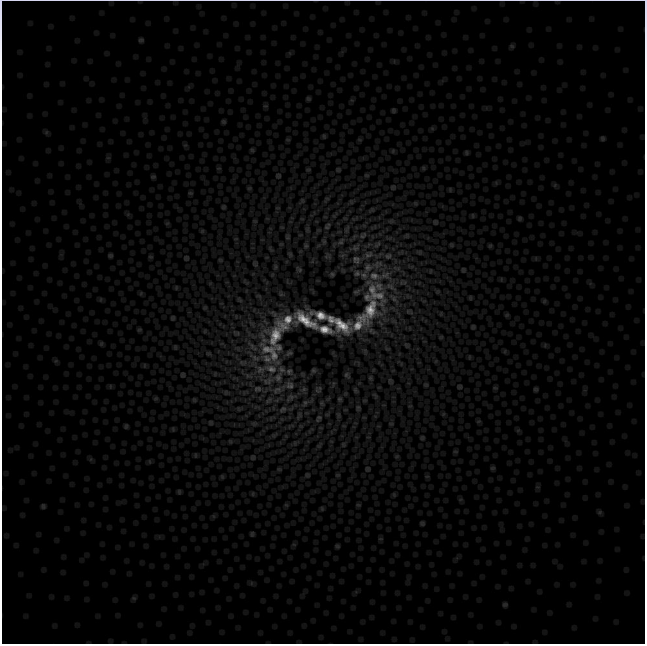

Figure : $t = 5$ million years for Spiral Galaxy Simulation #1.

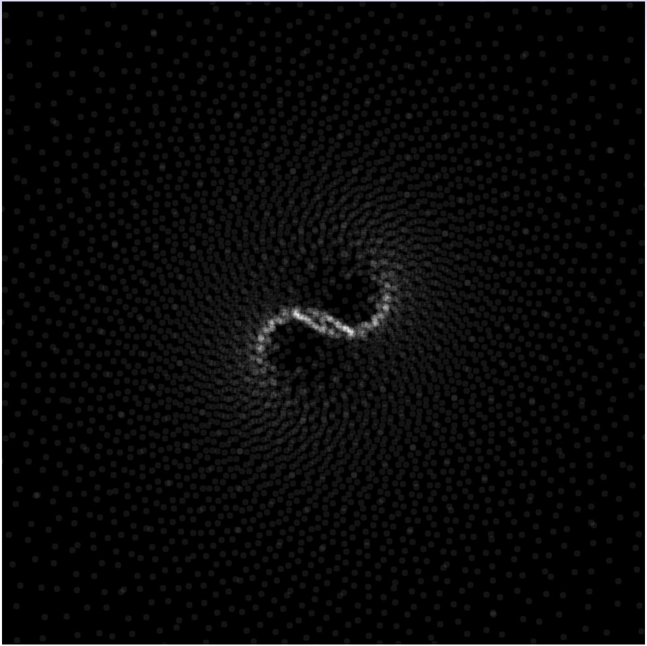

Figure : $t = 6$ million years for Spiral Galaxy Simulation #1.

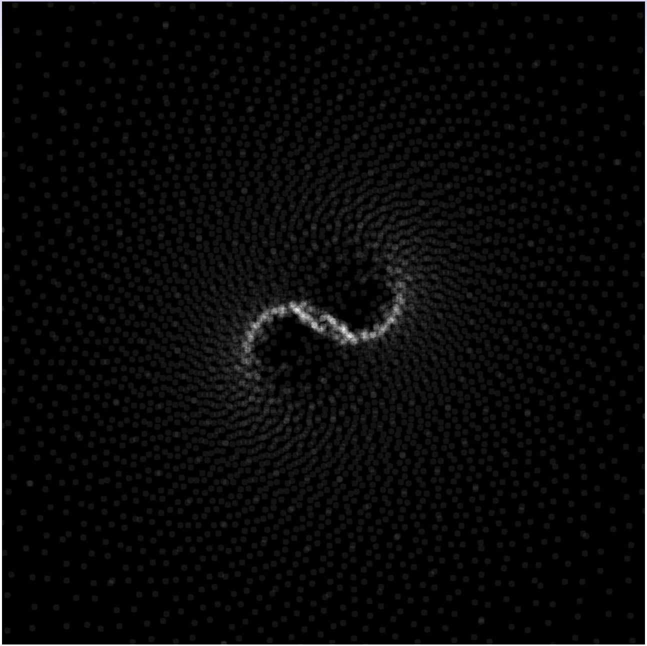

Figure : $t = 7$ million years for Spiral Galaxy Simulation #1.

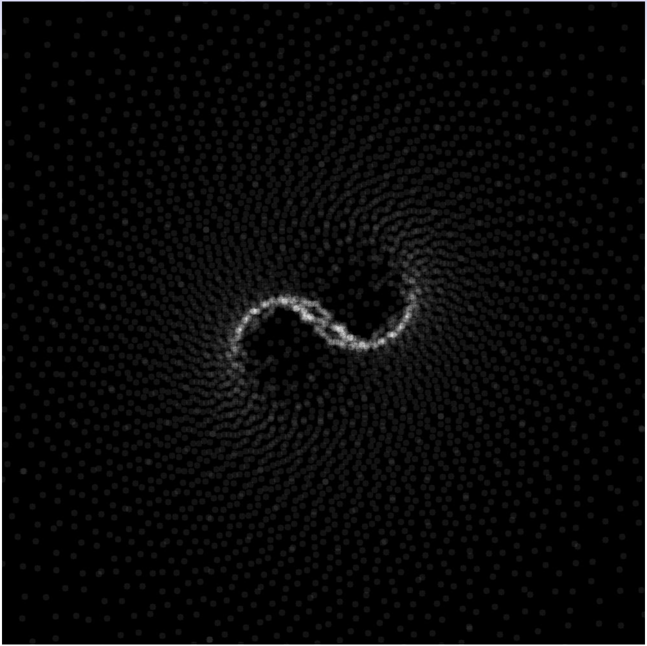

Figure : $t = 8$ million years for Spiral Galaxy Simulation #1.

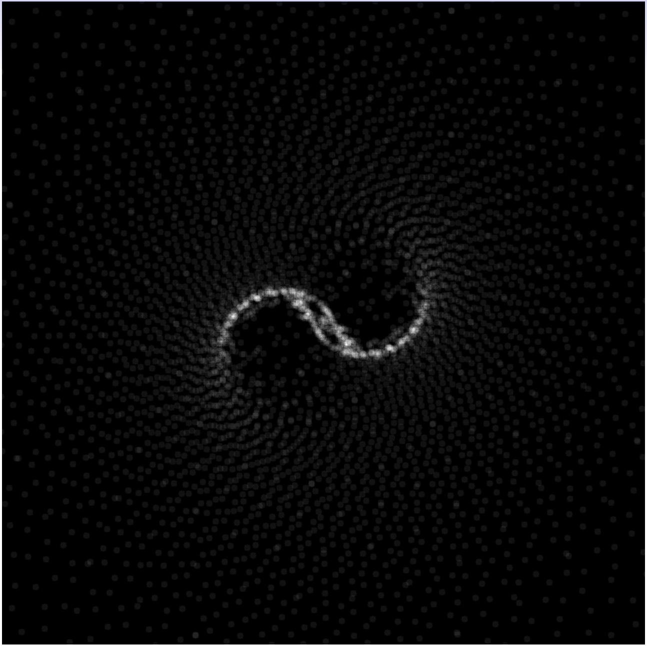

Figure : $t = 9$ million years for Spiral Galaxy Simulation #1.

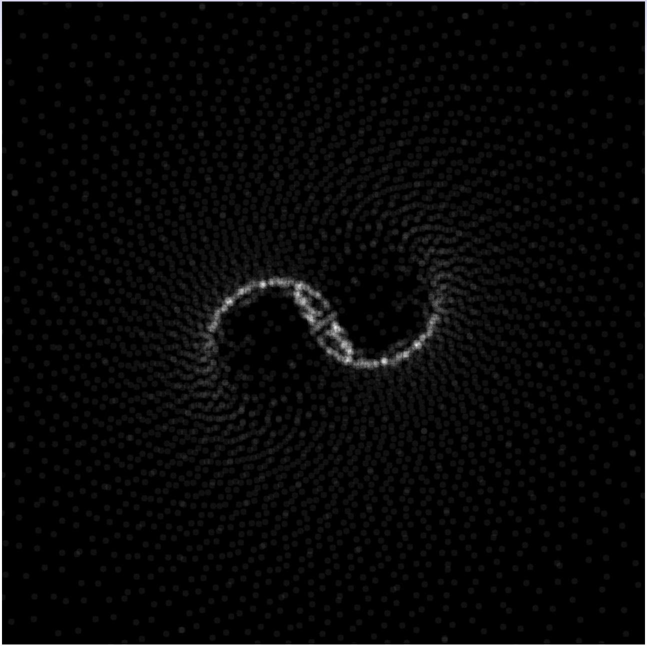

Figure : $t = 10$ million years for Spiral Galaxy Simulation #1.

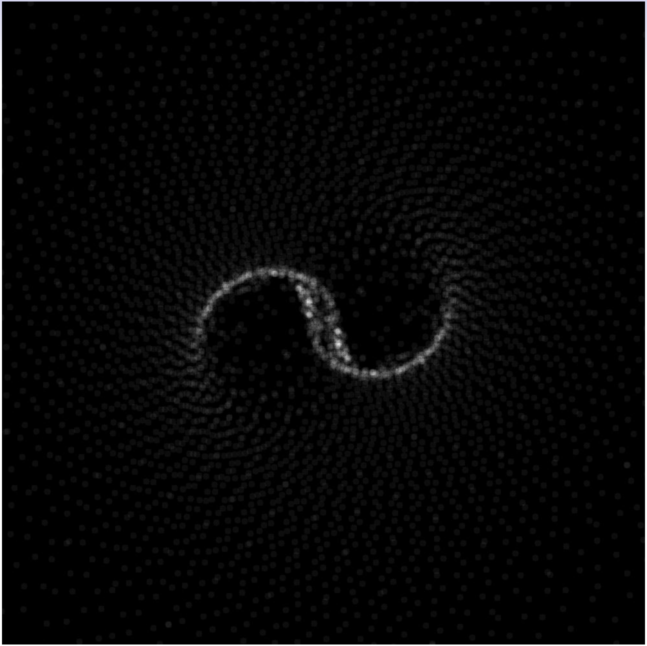

Figure : $t = 11$ million years for Spiral Galaxy Simulation #1.

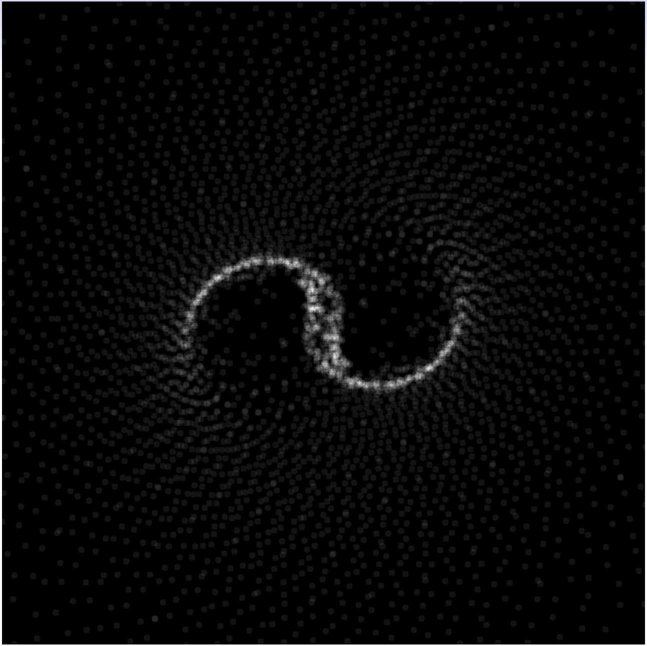

Figure : $t = 12$ million years for Spiral Galaxy Simulation #1.

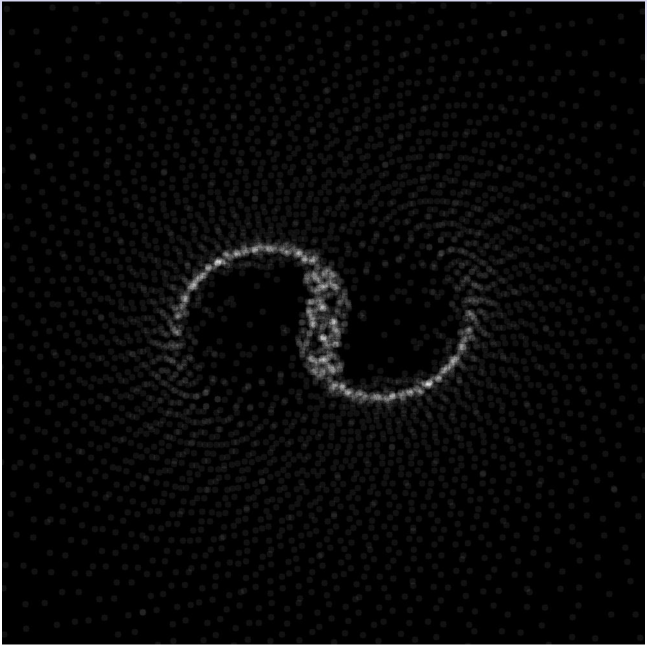

Figure : $t = 13$ million years for Spiral Galaxy Simulation #1.

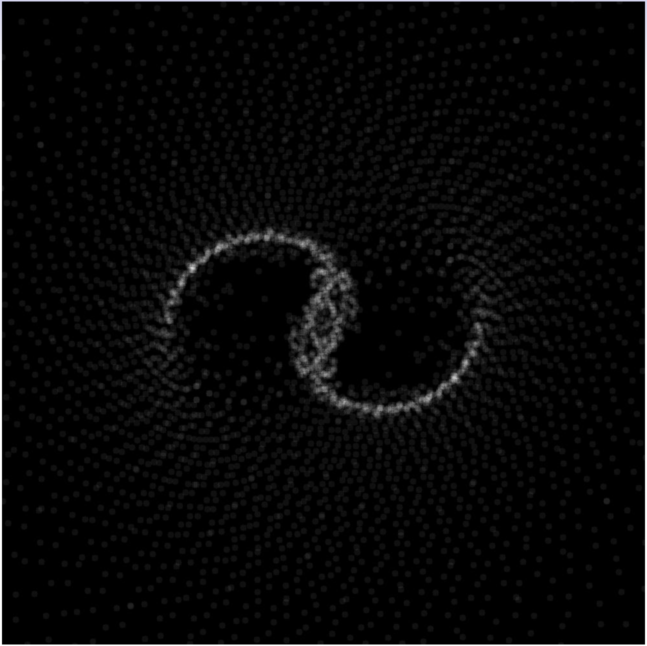

Figure : $t = 14$ million years for Spiral Galaxy Simulation $\#1$.

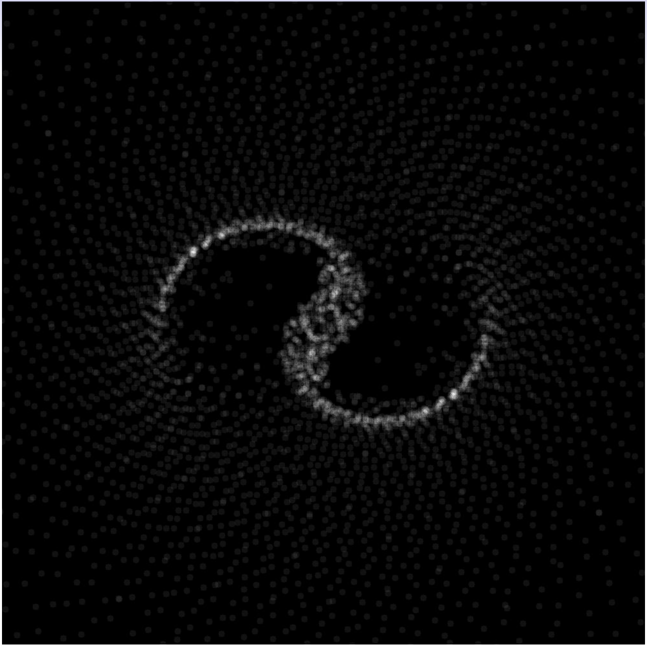

Figure : $t = 15$ million years for Spiral Galaxy Simulation #1.

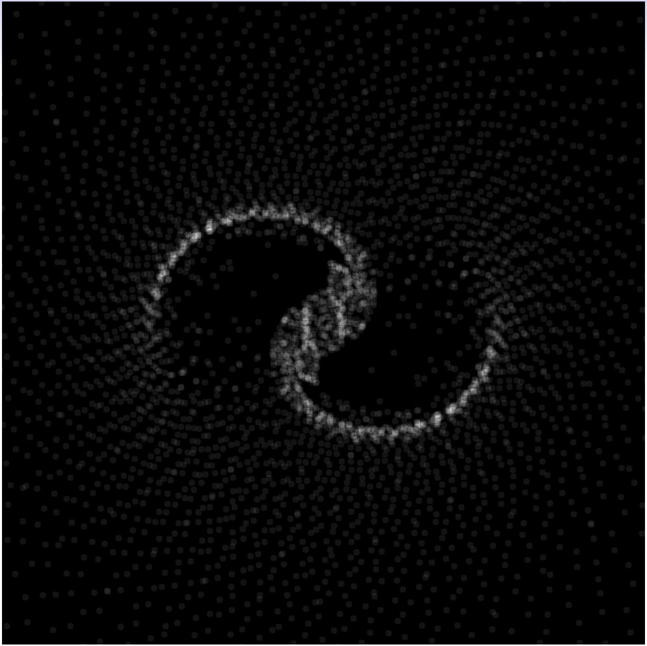

Figure : $t = 16$ million years for Spiral Galaxy Simulation #1.

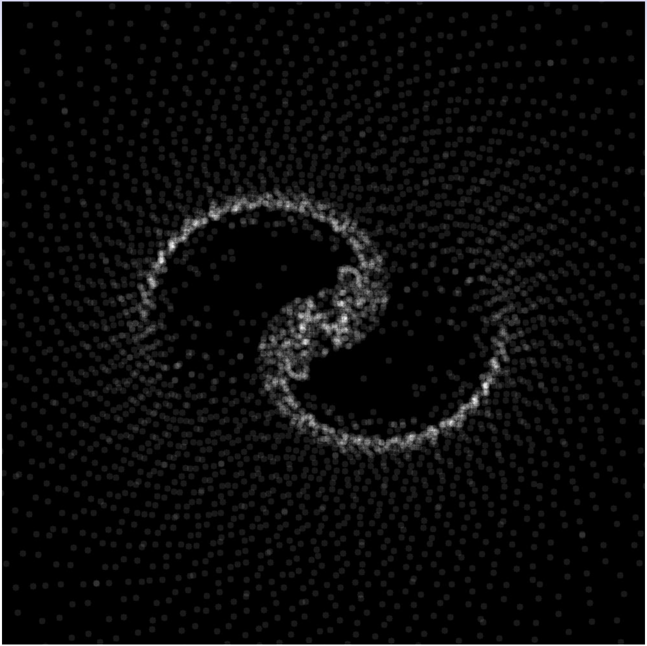

Figure : $t = 17$ million years for Spiral Galaxy Simulation #1.

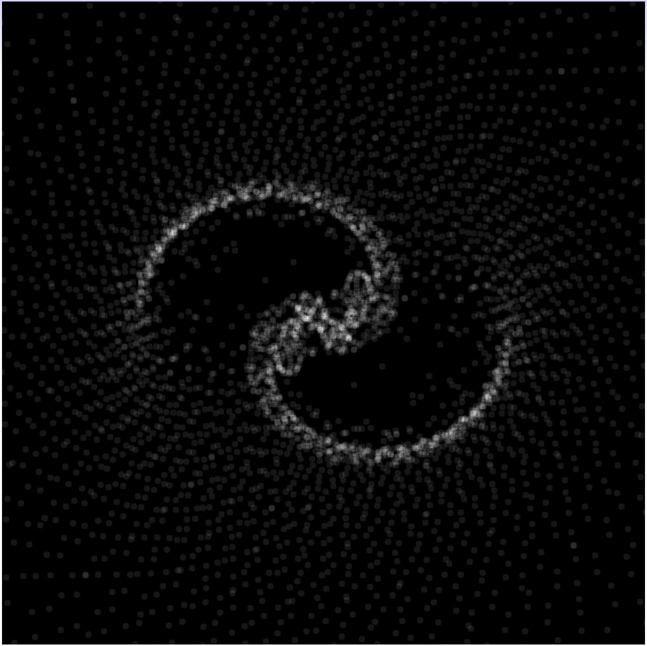

Figure : $t = 18$ million years for Spiral Galaxy Simulation #1.

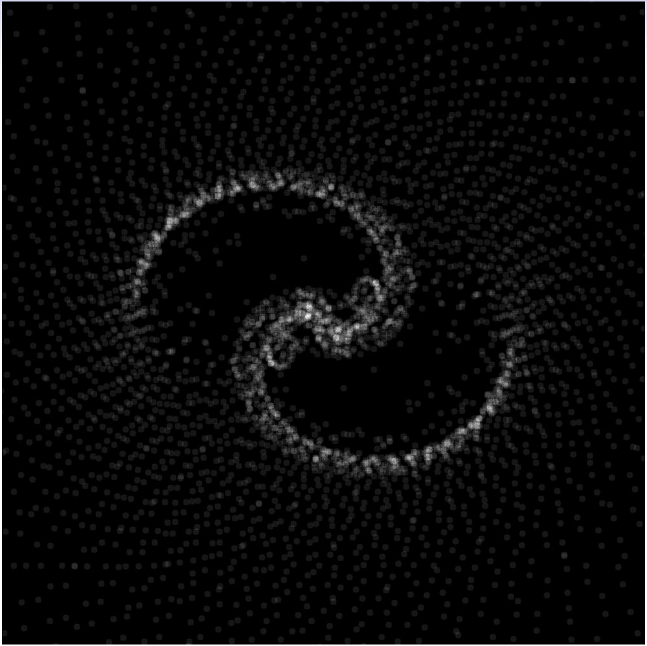

Figure : $t = 19$ million years for Spiral Galaxy Simulation $\#1$.

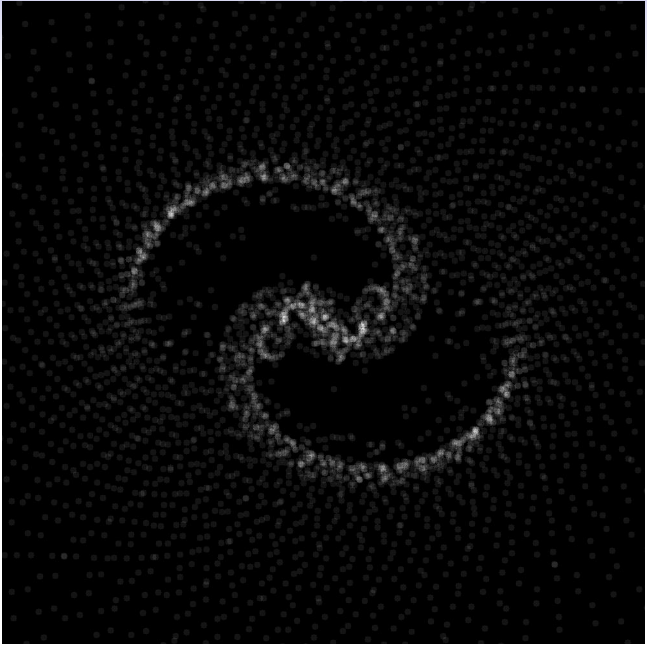

Figure : $t = 20$ million years for Spiral Galaxy Simulation $\#1$.

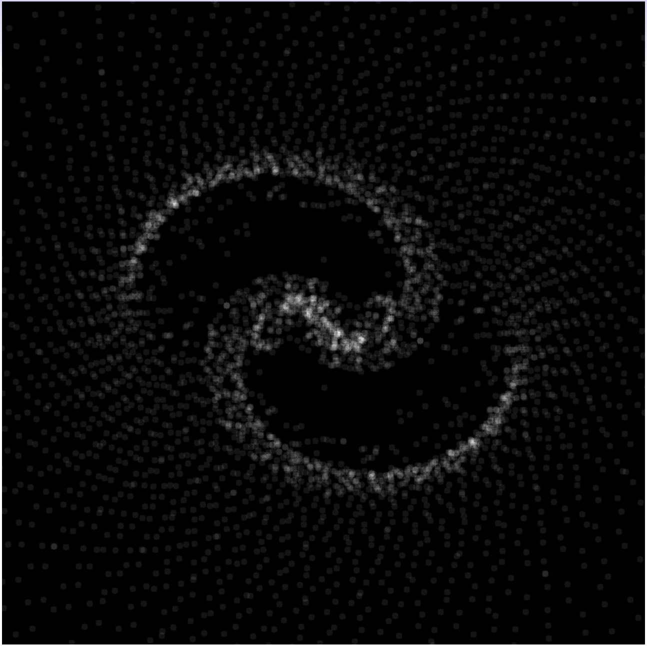

Figure : $t = 21$ million years for Spiral Galaxy Simulation #1.

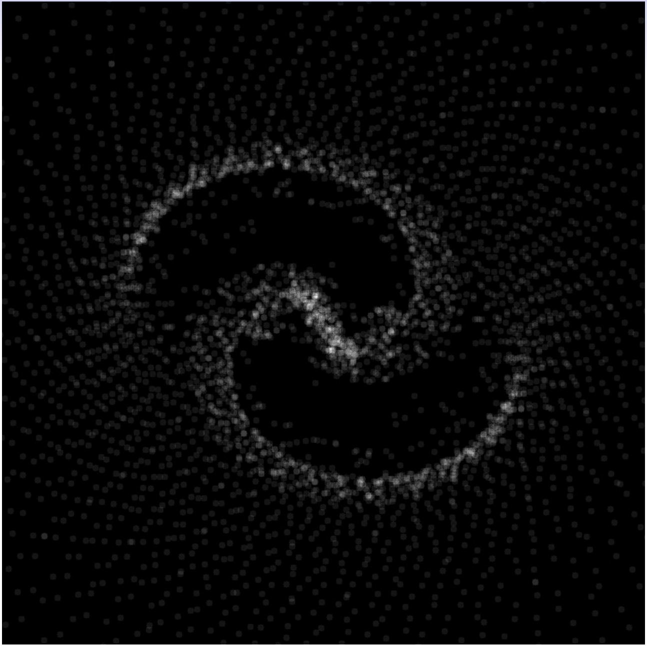

Figure : $t = 22$ million years for Spiral Galaxy Simulation #1.

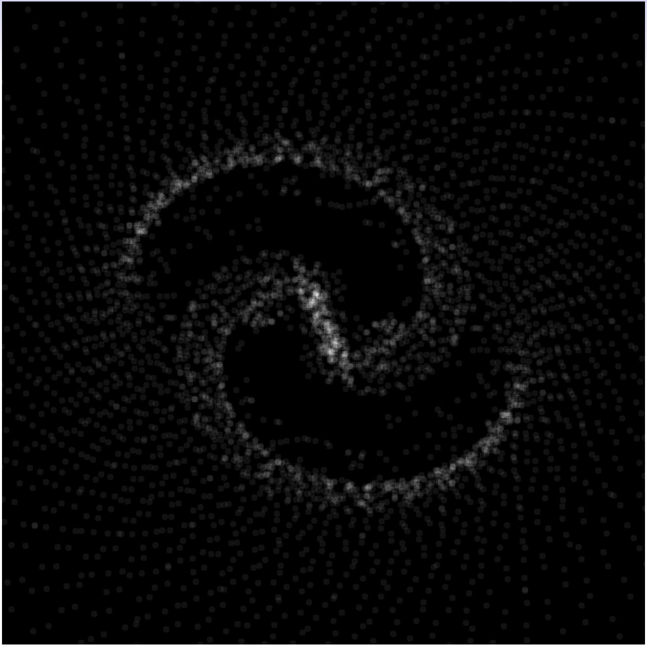

Figure : $t = 23$ million years for Spiral Galaxy Simulation $\#1$.

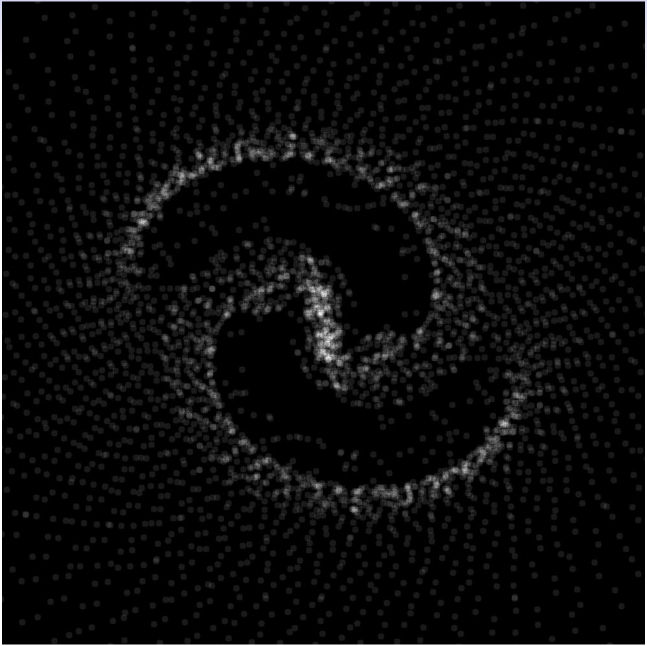

Figure : $t = 24$ million years for Spiral Galaxy Simulation $\#1$.

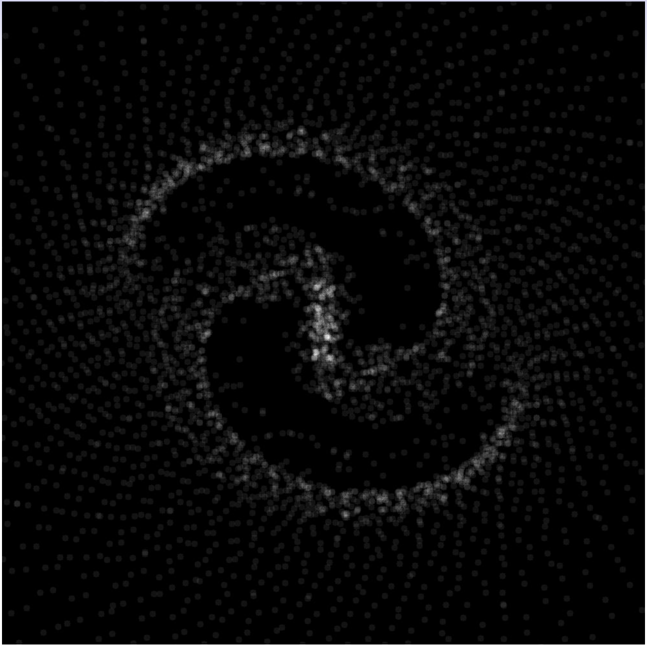

Figure : $t = 25$ million years for Spiral Galaxy Simulation #1.

Spiral Galaxy Simulation #1

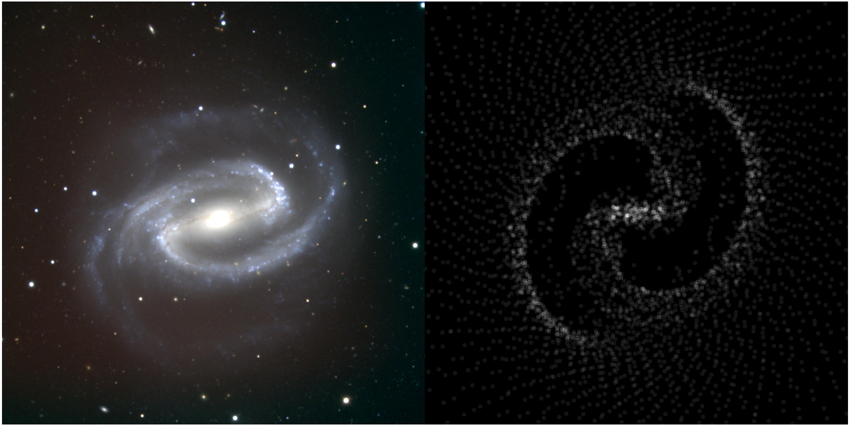

NGC1300 on the left, simulation on the right.

Spiral Galaxy Simulation #3

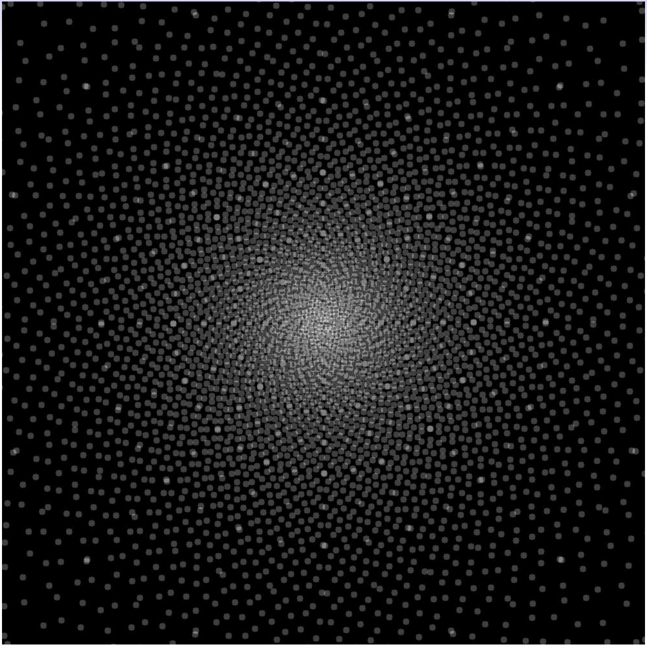

Figure : $t = 0$ million years for Spiral Galaxy Simulation #3.

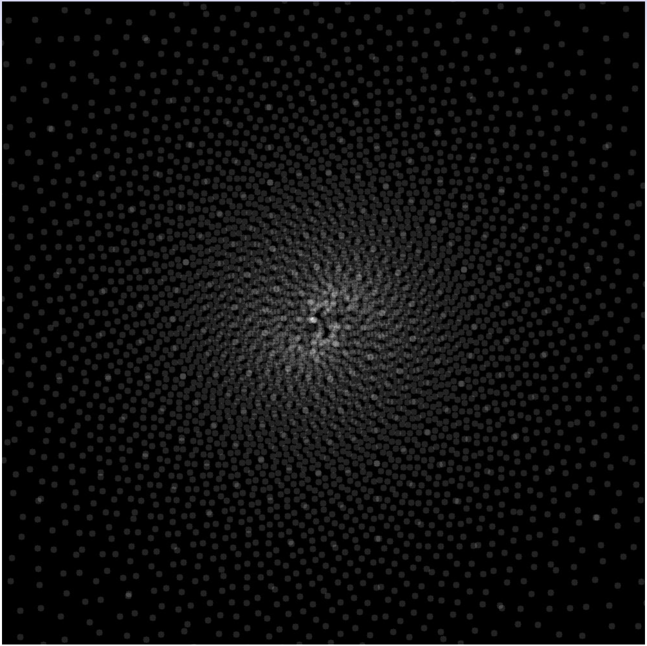

Figure : $t = 5$ million years for Spiral Galaxy Simulation #3.

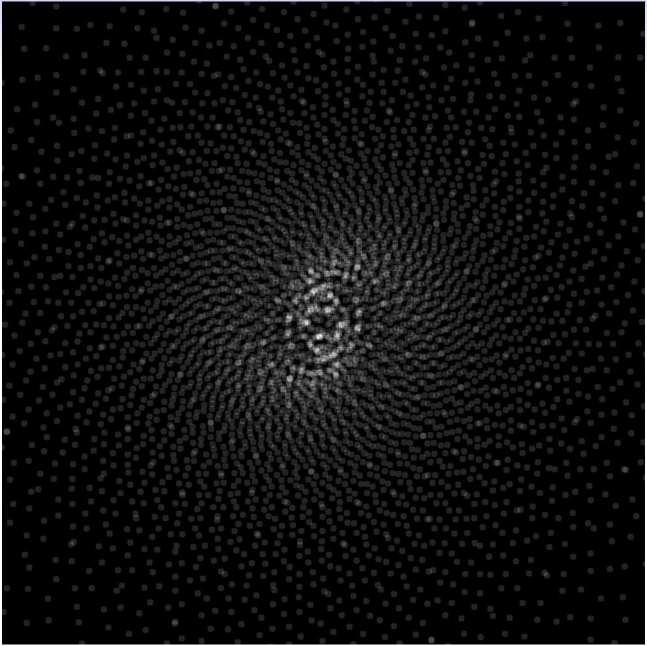

Figure : $t = 10$ million years for Spiral Galaxy Simulation #3.

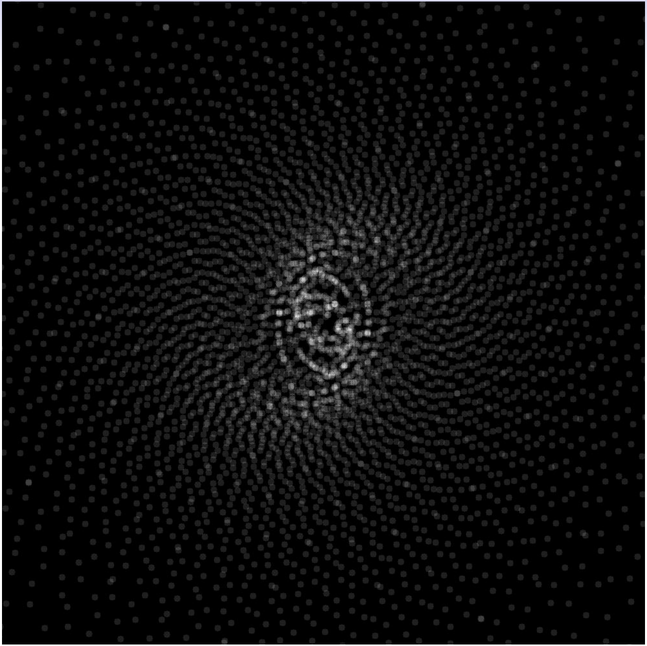

Figure : $t = 15$ million years for Spiral Galaxy Simulation #3.

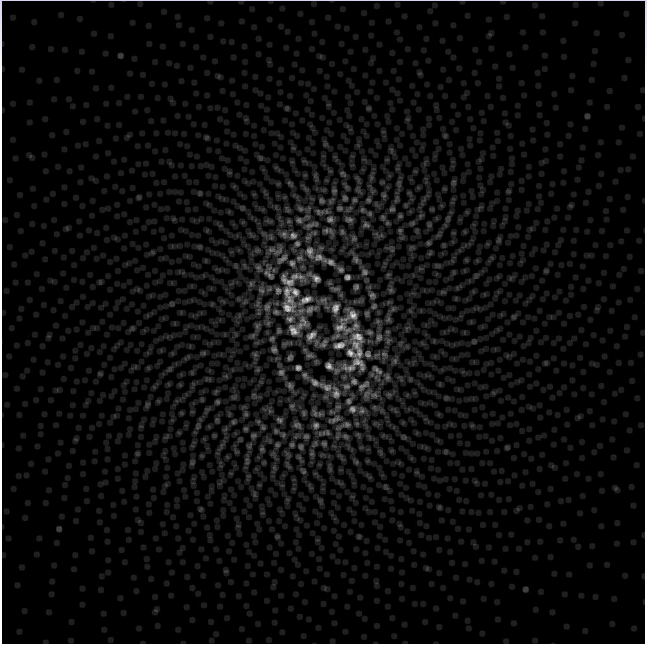

Figure : $t = 20$ million years for Spiral Galaxy Simulation $\#3$.

Figure : $t = 25$ million years for Spiral Galaxy Simulation $\#3$.

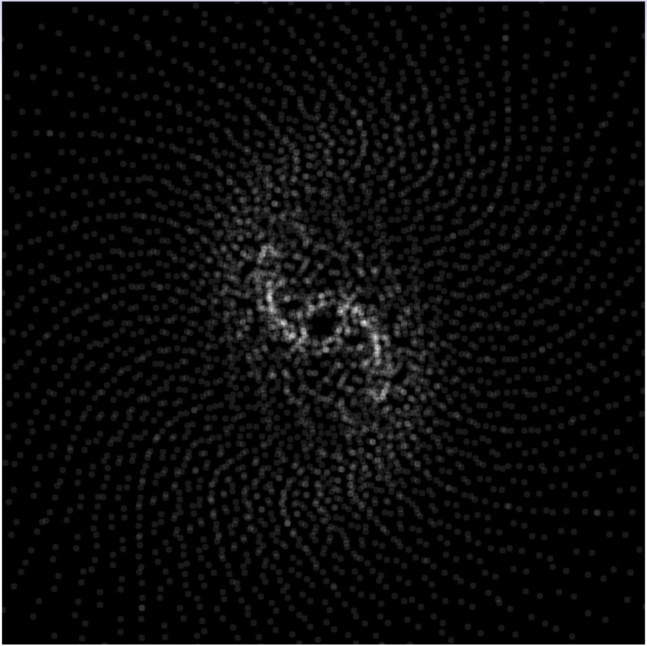

Figure : $t = 30$ million years for Spiral Galaxy Simulation #3.

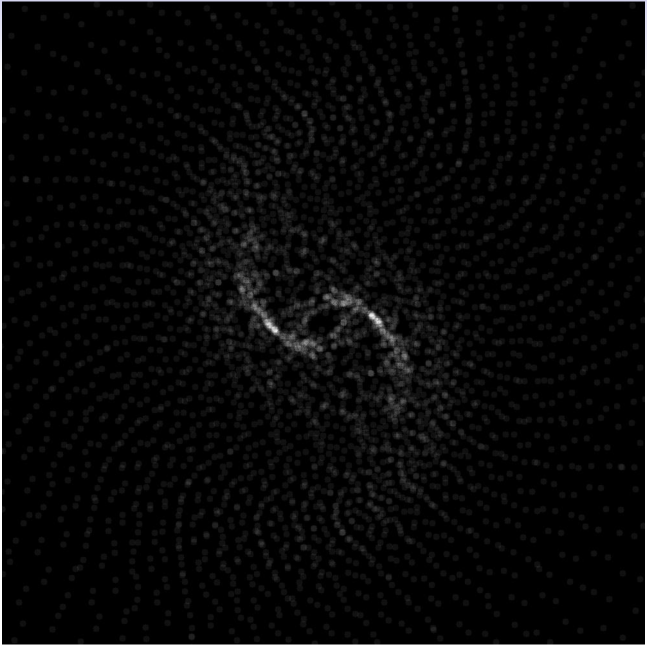

Figure : $t = 35$ million years for Spiral Galaxy Simulation #3.

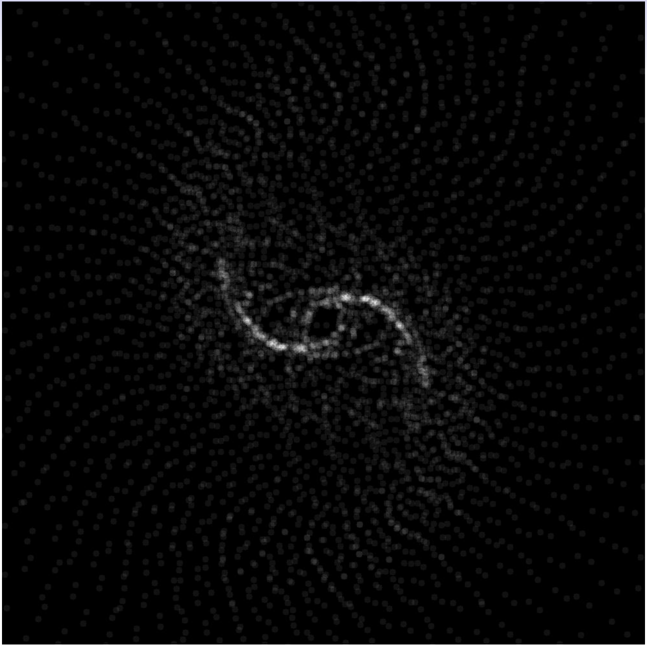

Figure : $t = 40$ million years for Spiral Galaxy Simulation #3.

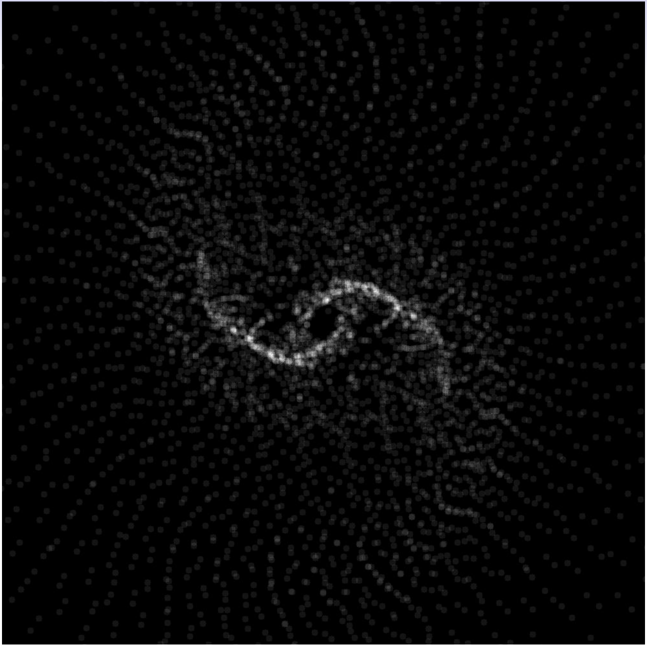

Figure : $t = 45$ million years for Spiral Galaxy Simulation #3.

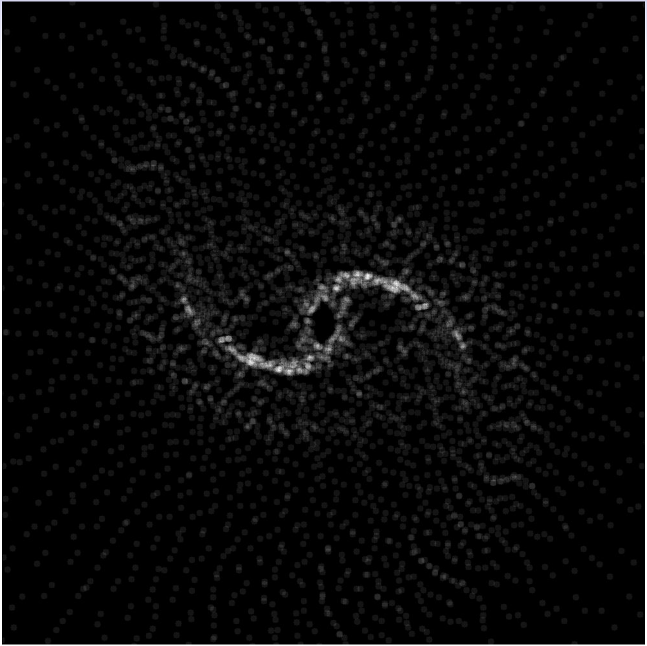

Figure : $t = 50$ million years for Spiral Galaxy Simulation #3.

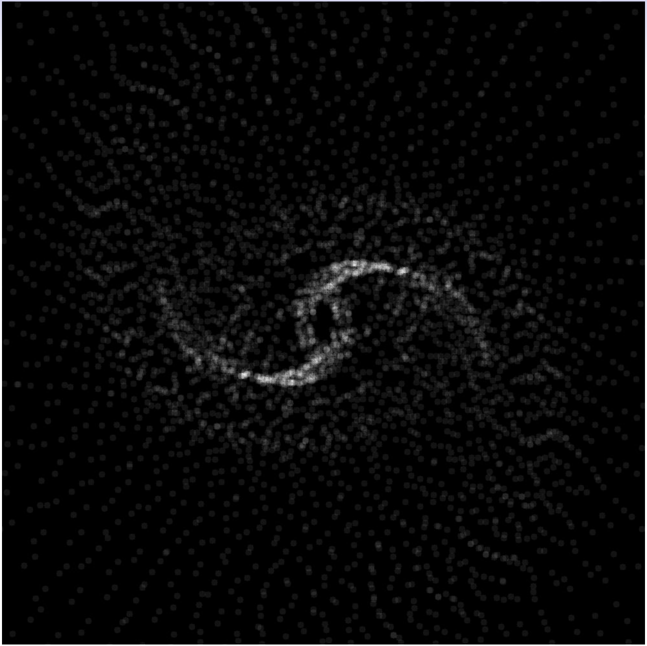

Figure : $t = 55$ million years for Spiral Galaxy Simulation #3.

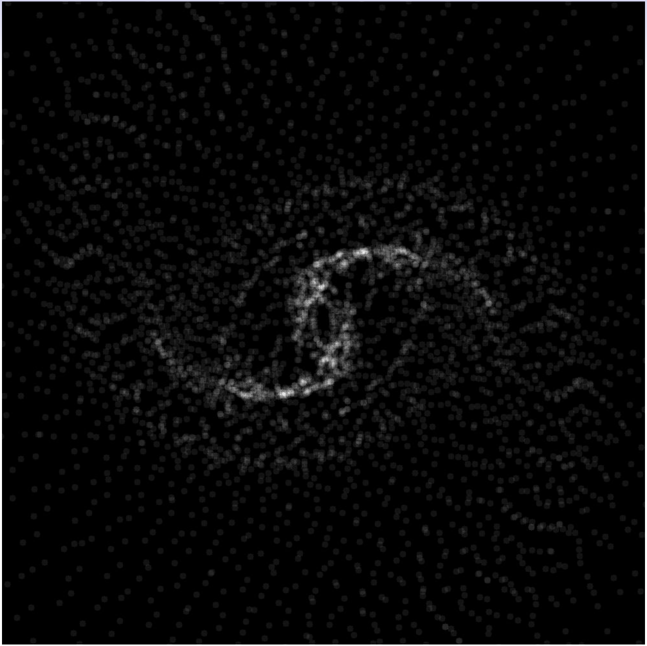

Figure : $t = 60$ million years for Spiral Galaxy Simulation #3.

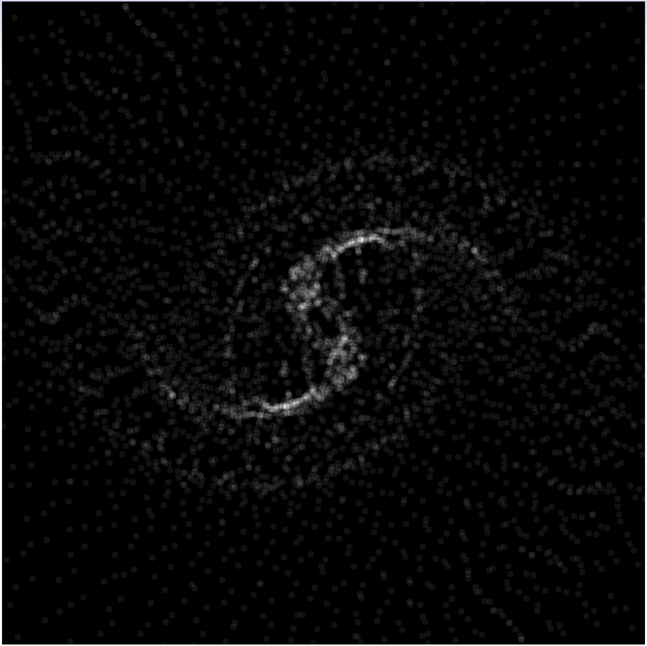

Figure : $t = 65$ million years for Spiral Galaxy Simulation #3.

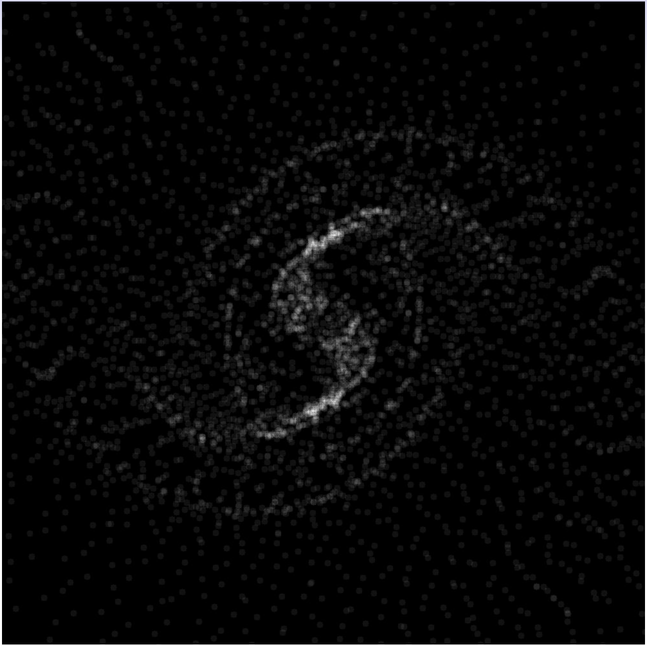

Figure : $t = 70$ million years for Spiral Galaxy Simulation #3.

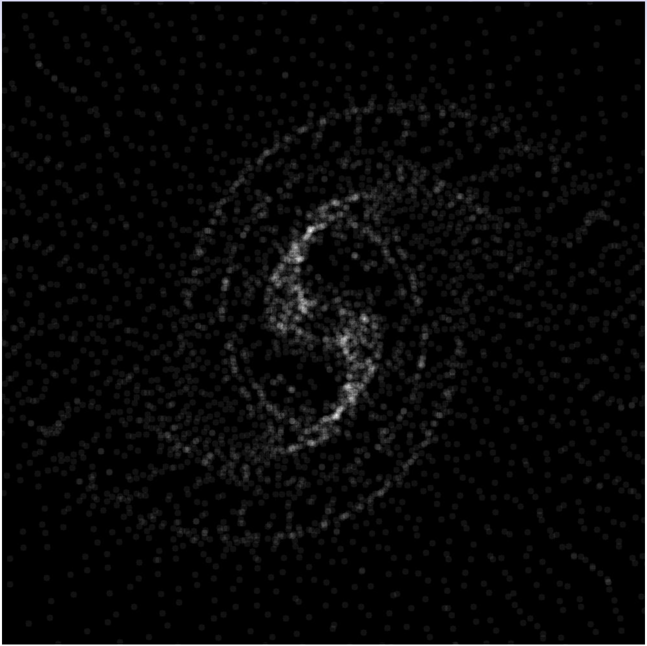

Figure : $t = 75$ million years for Spiral Galaxy Simulation #3.

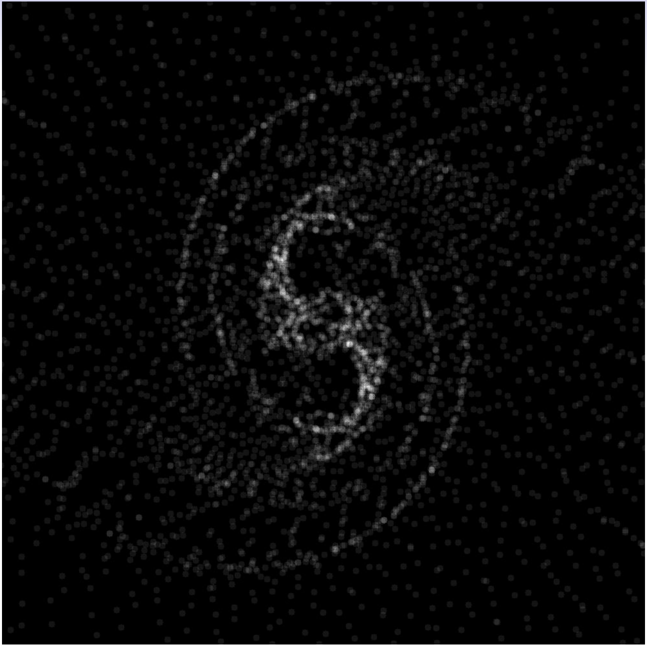

Figure : $t = 80$ million years for Spiral Galaxy Simulation #3.

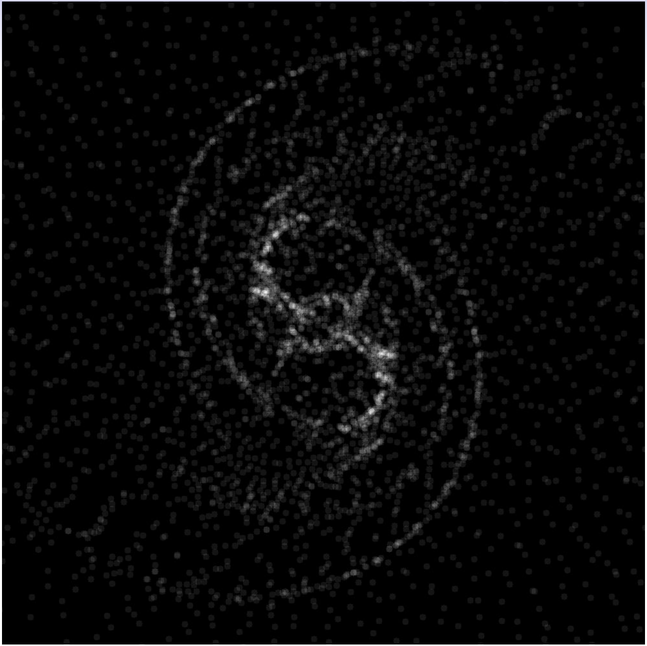

Figure : $t = 85$ million years for Spiral Galaxy Simulation $\#3$.

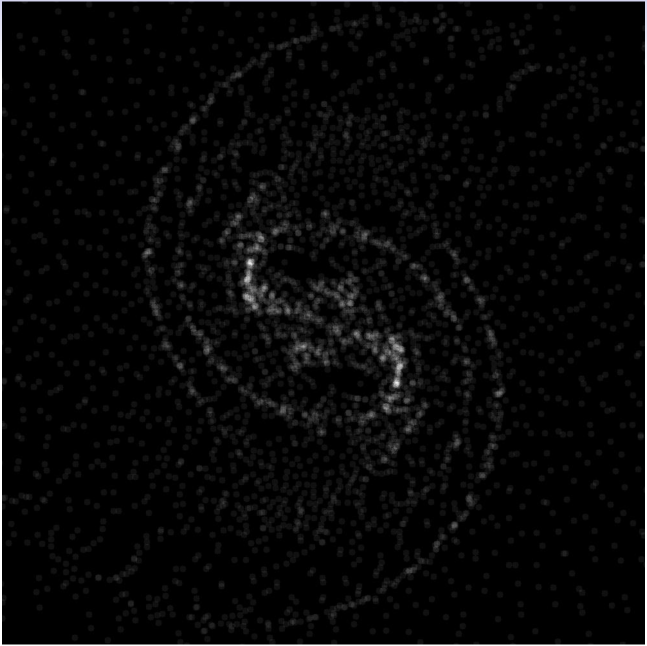

Figure : $t = 90$ million years for Spiral Galaxy Simulation #3.

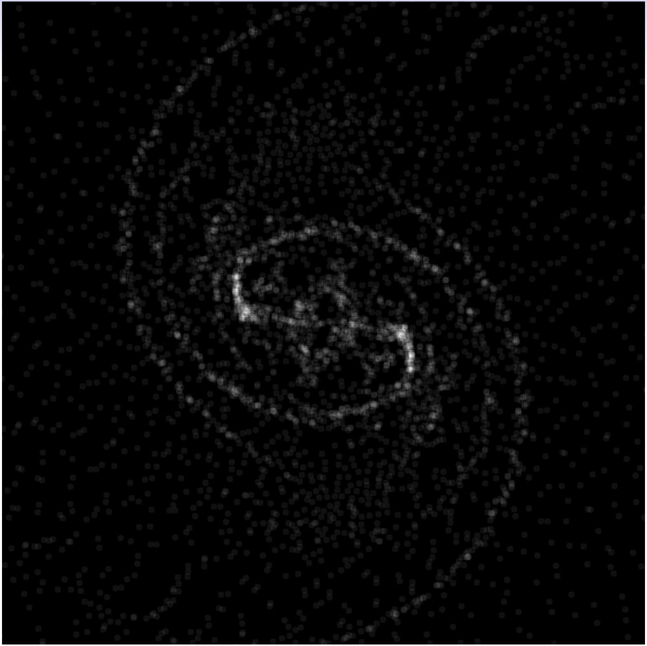

Figure : $t = 95$ million years for Spiral Galaxy Simulation #3.

Spiral Galaxy Simulation #3

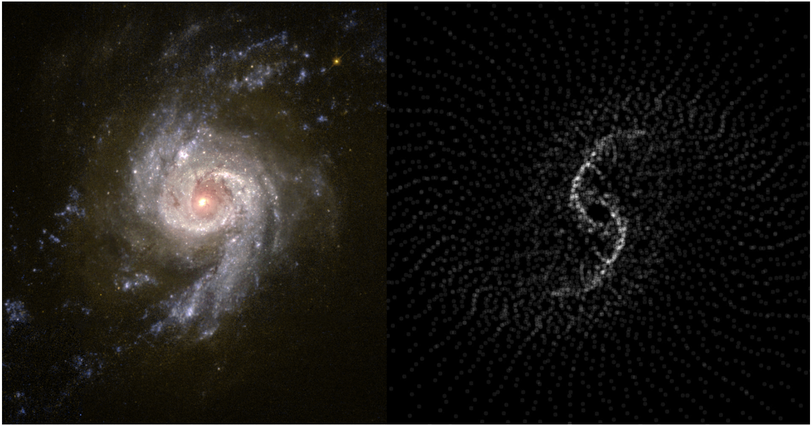

NGC3310 on the left, simulation on the right.

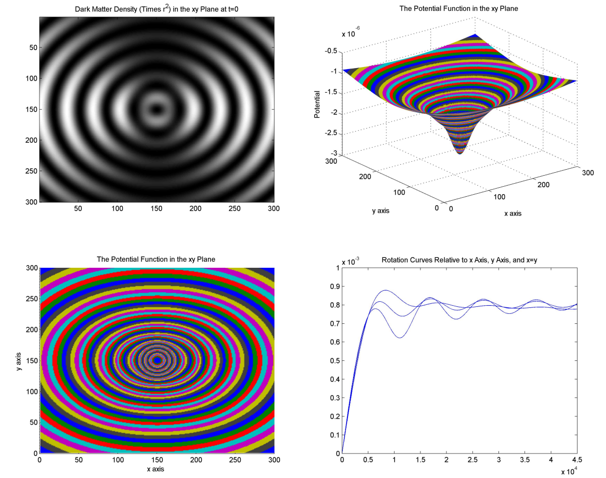

Figure : Spiral Galaxy Simulation #4: The dark matter density times r^2 in the xy plane (top left), the potential function in the xy plane (top right), the level sets of the potential function in the xy plane (bottom left), and the rotation curve (bottom right), all to a radius of $45,000$ light years.

Spiral Galaxy Simulation #4

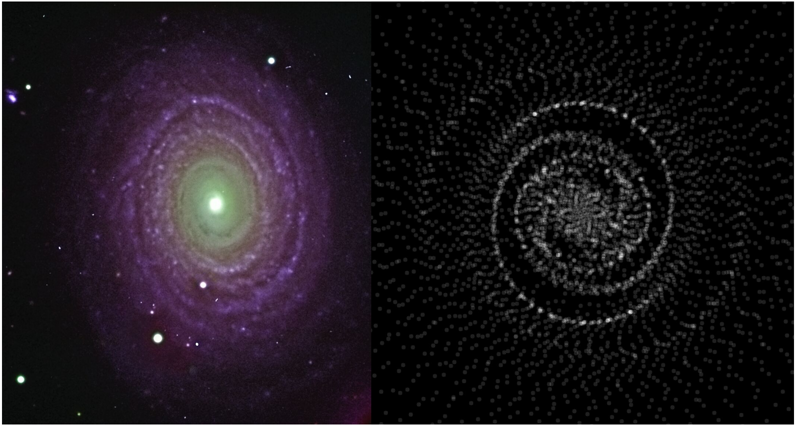

NGC488 on the left, simulation on the right.

Elliptical Galaxies

Figure : Elliptical galaxies contain ellipsoidal shaped collections of stars in mostly radial orbits. Two examples are M87 (left) and NGC1132 (right).

Ripples in the Brightness Profiles of Elliptical Galaxies

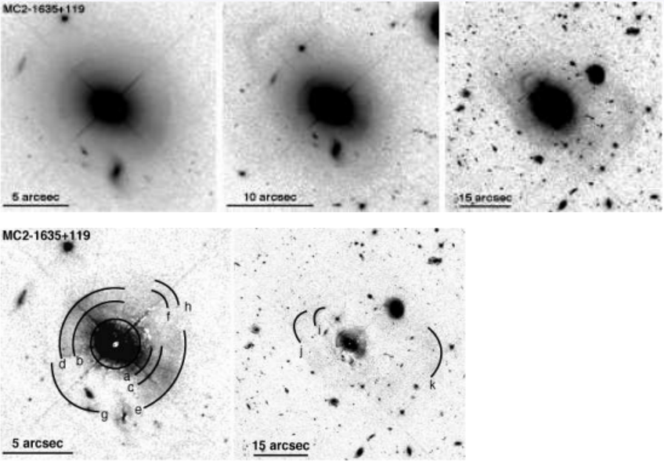

Figure : From "Spectacular Shells in the Host Galaxy of the QSO MC2 1635+119" by Canalizo, Bennert, Jungwiert, Stockton, Schweizer, Lacy, Peng (2007), Astrophysics Journal and on the arXiv.

Ripples in the Brightness Profiles of Elliptical Galaxies

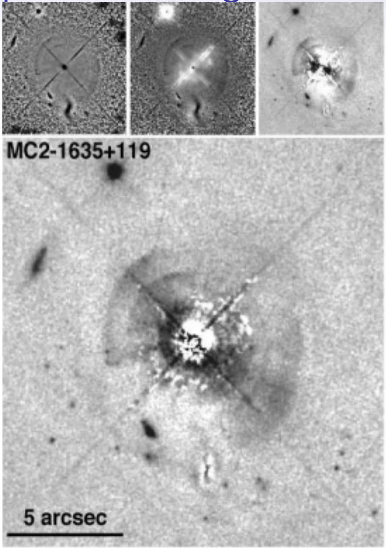

Do these ripples come from a degree 1 spherical harmonic component to the dark matter scalar field solution to the Klein-Gordon equation?

Ripples in the Brightness Profiles of Elliptical Galaxies

Between 10% and 20% of all elliptical galaxies are found to contain sharp steps in their luminosity profiles like those just shown. These features are called ripples or shells and have been observed since 1980.

In *Galactic Astronomy* (1999), Binney and Merrifield write:

"...the existence of ripples directly challenges the classical picture of ellipticals. ...simulations have successfully reproduced the interleaved property of ripples ... Despite these successes significant uncertainties still surround the ripple phenomenon because the available simulations have important limitations, and it is not clear how probable their initial conditions are."

Ripples in the Brightness Profiles of Elliptical Galaxies

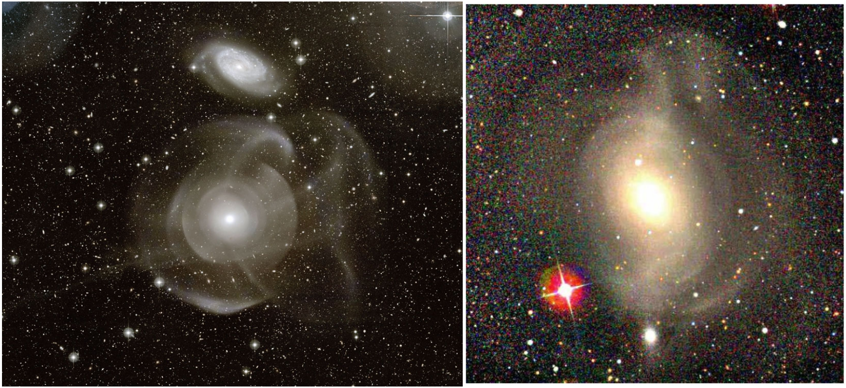

Figure : NGC474 on the left, NGC4382 on the right have unusually prominent concentric shells, also known as ripples, in their images.

Ripples in the Brightness Profiles of Elliptical Galaxies

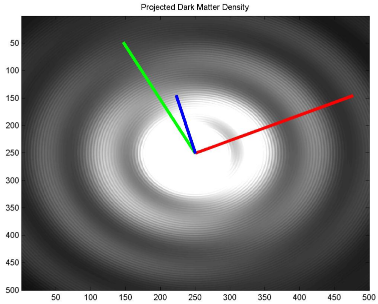

Figure : Projected wave dark matter density. Wave dark matter may offer another possibility to explain ripples in elliptical galaxies, but more study is required.

Ripples in the Brightness Profiles of Elliptical Galaxies

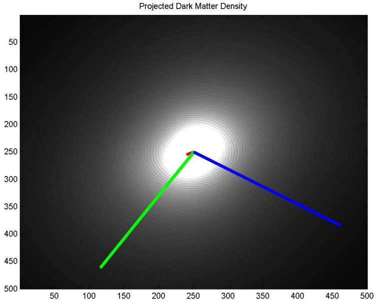

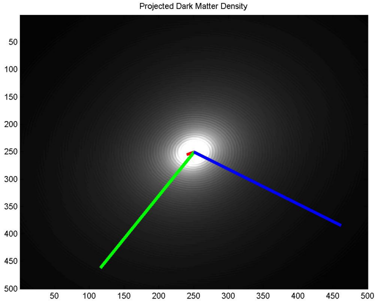

Figure : Same wave dark matter density, but viewed from a different angle where the ripples are not visible.

Dwarf Spheroidal Galaxies

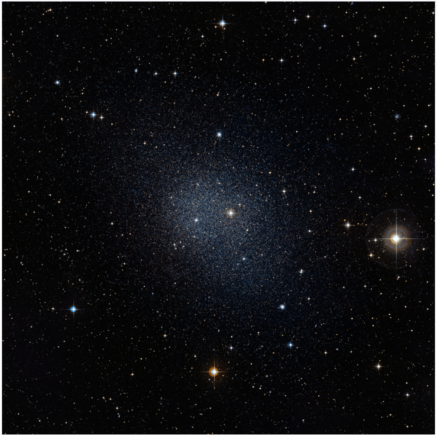

Fornax Dwarf Spheroidal Galaxy. Photo Credit: ESO/Digital Sky Survey 2

Approximately spherically symmetric, and
almost entirely dark matter, over 99% in some cases.

Working Value of Υ (joint with Alan Parry)

- For $\Upsilon = 50$ yr^{-1}, there exists at least one n^{th} excited state dark matter mass profile for some $n \leq 3$ which is qualitatively similar to the Burkert dark matter mass profile found by Salucci et al. for each of the classical dwarf spheroidal galaxies.

3^{rd} Excited State

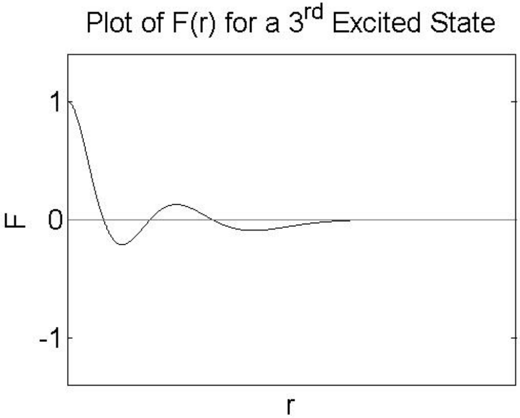

Plot of the scalar field F in a
static spherically symmetric 3^{rd} excited state.

3^{rd} Excited State

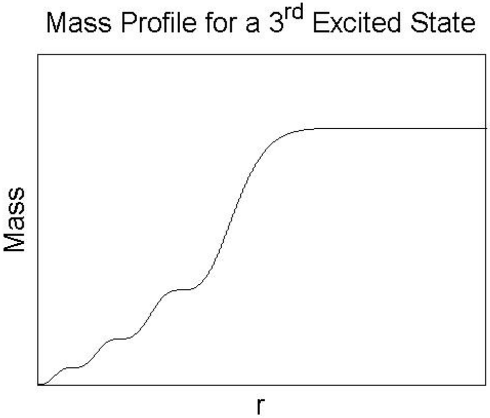

Plot of the mass M in a
static spherically symmetric 3^{rd} excited state.

$\Upsilon = 50 \text{ yr}^{-1}$

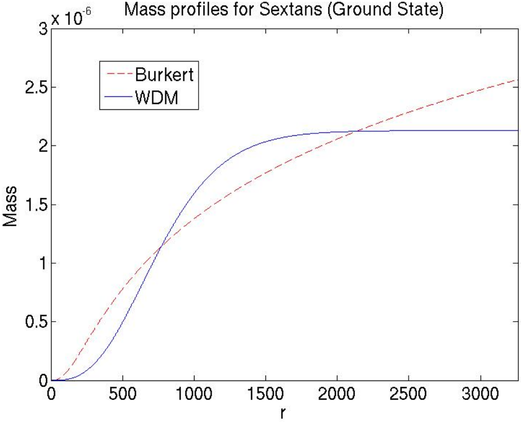

$\Upsilon = 50 \text{ yr}^{-1}$

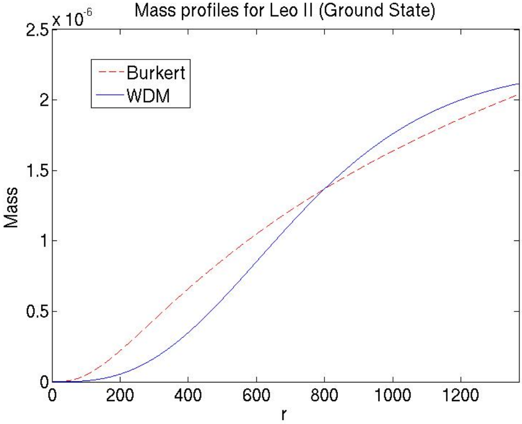

$\Upsilon = 50\ \mathrm{yr}^{-1}$

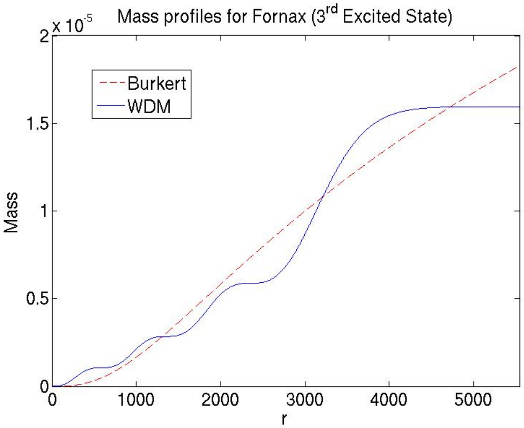

$\Upsilon = 50\ \mathrm{yr}^{-1}$

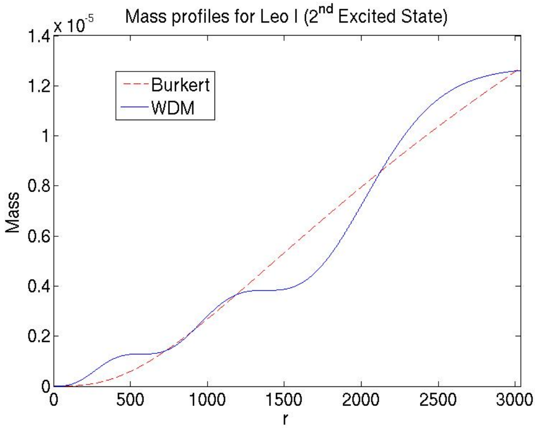

$\Upsilon = 50\ \text{yr}^{-1}$

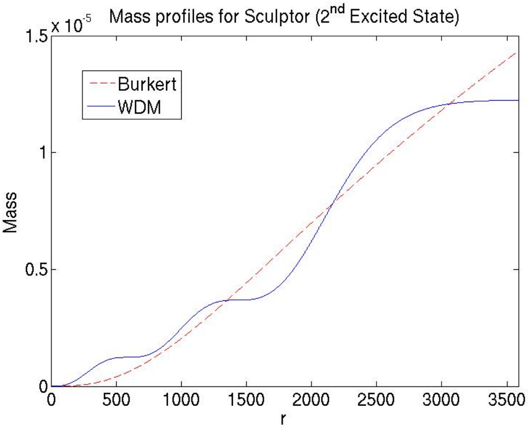

$\Upsilon = 50\ \mathrm{yr}^{-1}$

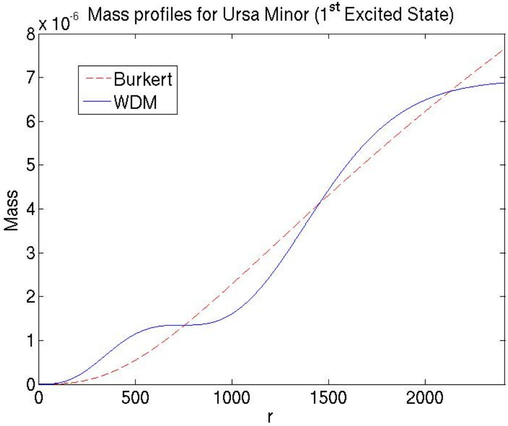

$\Upsilon = 50 \text{ yr}^{-1}$

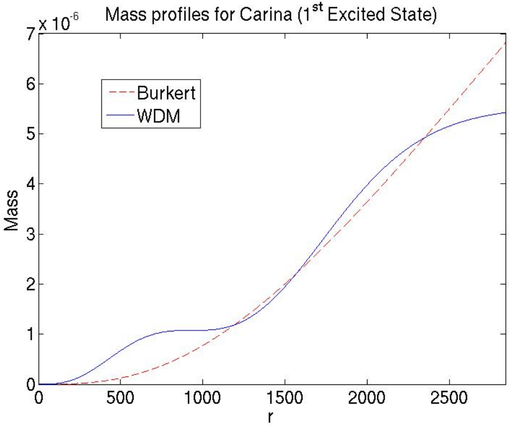

$\Upsilon = 50\ \mathrm{yr}^{-1}$

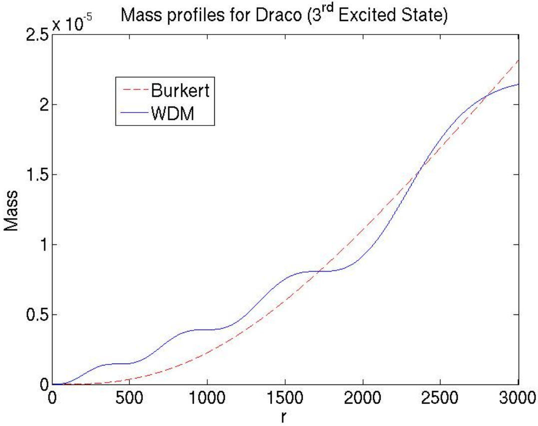

Upper Bounds on Υ

Galaxy \ State	0	1	2	3
Sextans	$\Upsilon < 160$	$\Upsilon < 394$	$\Upsilon < 633$	$\Upsilon < 875$
Leo II	$\Upsilon < 234$	$\Upsilon < 576$	$\Upsilon < 926$	$\Upsilon < 1279$
Fornax	$\Upsilon < 35$	$\Upsilon < 87$	$\Upsilon < 139$	$\Upsilon < 192$
Leo I	$\Upsilon < 57$	$\Upsilon < 141$	$\Upsilon < 226$	$\Upsilon < 312$
Sculptor	$\Upsilon < 49$	$\Upsilon < 121$	$\Upsilon < 194$	$\Upsilon < 268$
Ursa Minor	$\Upsilon < 82$	$\Upsilon < 202$	$\Upsilon < 325$	$\Upsilon < 449$
Carina	$\Upsilon < 84$	$\Upsilon < 207$	$\Upsilon < 333$	$\Upsilon < 459$
Draco	$\Upsilon < 45$	$\Upsilon < 111$	$\Upsilon < 179$	$\Upsilon < 246$

Galaxy \ State	4	5	10	20
Sextans	$\Upsilon < 1116$	$\Upsilon < 1356$	$\Upsilon < 2460$	$\Upsilon < 4789$
Leo II	$\Upsilon < 1632$	$\Upsilon < 1983$	$\Upsilon < 3597$	$\Upsilon < 7003$
Fornax	$\Upsilon < 245$	$\Upsilon < 297$	$\Upsilon < 538$	$\Upsilon < 1048$
Leo I	$\Upsilon < 398$	$\Upsilon < 484$	$\Upsilon < 877$	$\Upsilon < 1706$
Sculptor	$\Upsilon < 342$	$\Upsilon < 416$	$\Upsilon < 754$	$\Upsilon < 1467$
Ursa Minor	$\Upsilon < 572$	$\Upsilon < 695$	$\Upsilon < 1261$	$\Upsilon < 2455$
Carina	$\Upsilon < 586$	$\Upsilon < 712$	$\Upsilon < 1292$	$\Upsilon < 2514$
Draco	$\Upsilon < 314$	$\Upsilon < 382$	$\Upsilon < 692$	$\Upsilon < 1347$

Summary of Dwarf Spheroidal Galaxy Results (joint with Alan Parry)

Conclusion 1 For $\Upsilon = 50$ yr^{-1}, there exists at least one n^{th} excited state dark matter mass profile for some $n \leq 3$ which is qualitatively similar to the Burkert dark matter mass profile found by Salucci et al. for each of the classical dwarf spheroidal galaxies.

Summary of Dwarf Spheroidal Galaxy Results (joint with Alan Parry)

Conclusion 1 For $\Upsilon = 50$ yr^{-1}, there exists at least one n^{th} excited state dark matter mass profile for some $n \leq 3$ which is qualitatively similar to the Burkert dark matter mass profile found by Salucci et al. for each of the classical dwarf spheroidal galaxies.

Conclusion 2 Under a precise criteria to reject values of Υ as untenable, if the dark matter mass in all eight dwarf spheroidal galaxies are correctly modeled by a 20^{th} excited state or less, then $\Upsilon < 1000$ yr^{-1}.

Potential Arguments in Favor of Wave Dark Matter

1. Predicts that the dark matter in a homogeneous, isotropic universe should be cold, as observed.

Potential Arguments in Favor of Wave Dark Matter

1. Predicts that the dark matter in a homogeneous, isotropic universe should be cold, as observed.
2. Might explain why there may be a rough lower bound on the mass of isolated blobs of dark matter (dwarf spheroidal galaxies).

Potential Arguments in Favor of Wave Dark Matter

1. Predicts that the dark matter in a homogeneous, isotropic universe should be cold, as observed.
2. Might explain why there may be a rough lower bound on the mass of isolated blobs of dark matter (dwarf spheroidal galaxies).
3. Predicts bounded dark matter density in the cores of galaxies, unlike WIMP dark matter which may predict cusps as in the Navarro-Frenk-White profile (still unobserved).

Potential Arguments in Favor of Wave Dark Matter

1. Predicts that the dark matter in a homogeneous, isotropic universe should be cold, as observed.
2. Might explain why there may be a rough lower bound on the mass of isolated blobs of dark matter (dwarf spheroidal galaxies).
3. Predicts bounded dark matter density in the cores of galaxies, unlike WIMP dark matter which may predict cusps as in the Navarro-Frenk-White profile (still unobserved).
4. Might explain spiral and barred spiral patterns in disk galaxies.

Potential Arguments in Favor of Wave Dark Matter

1. Predicts that the dark matter in a homogeneous, isotropic universe should be cold, as observed.
2. Might explain why there may be a rough lower bound on the mass of isolated blobs of dark matter (dwarf spheroidal galaxies).
3. Predicts bounded dark matter density in the cores of galaxies, unlike WIMP dark matter which may predict cusps as in the Navarro-Frenk-White profile (still unobserved).
4. Might explain spiral and barred spiral patterns in disk galaxies.
5. Might explain the interleaved shells seen in the brightness profiles of some elliptical galaxies.

Potential Arguments in Favor of Wave Dark Matter

1. Predicts that the dark matter in a homogeneous, isotropic universe should be cold, as observed.
2. Might explain why there may be a rough lower bound on the mass of isolated blobs of dark matter (dwarf spheroidal galaxies).
3. Predicts bounded dark matter density in the cores of galaxies, unlike WIMP dark matter which may predict cusps as in the Navarro-Frenk-White profile (still unobserved).
4. Might explain spiral and barred spiral patterns in disk galaxies.
5. Might explain the interleaved shells seen in the brightness profiles of some elliptical galaxies.

Much more study is required to settle these fascinating questions.

The Baryonic Tully-Fisher Relation

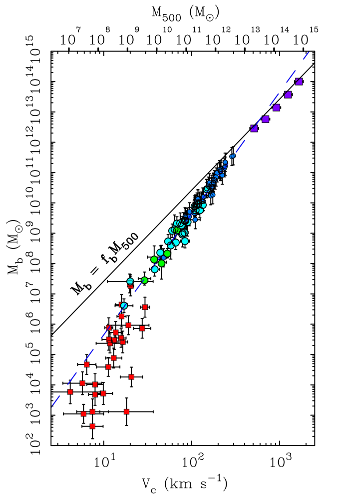

Figure : Total baryonic (regular) mass versus circular velocity. Each point represents a galaxy, including star dominated spirals (dark blue), gas dominated disks (light blue and green), Local Group dwarf satellites (red squares), except that the purple squares represent the mean of many galaxy clusters.

The Baryonic Tully-Fisher Relation

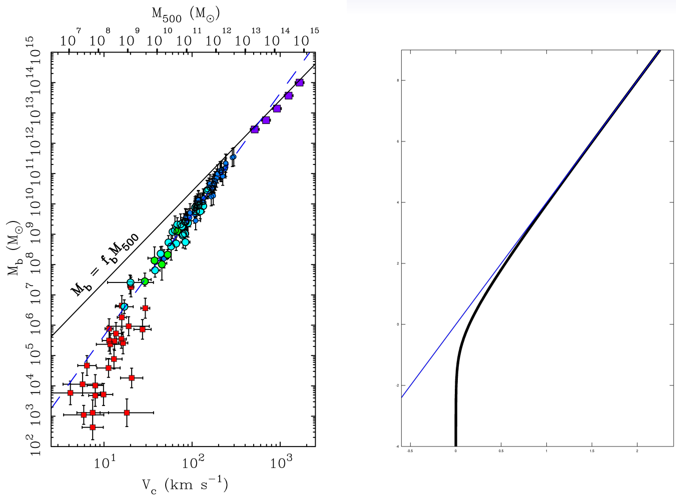

Figure : Total baryonic (regular) mass versus circular velocity. Each point represents a galaxy, including star dominated spirals (dark blue), gas dominated disks (light blue and green), Local Group dwarf satellites (red squares), except that the purple squares represent the mean of many galaxy clusters.

The Baryonic Tully-Fisher Relation

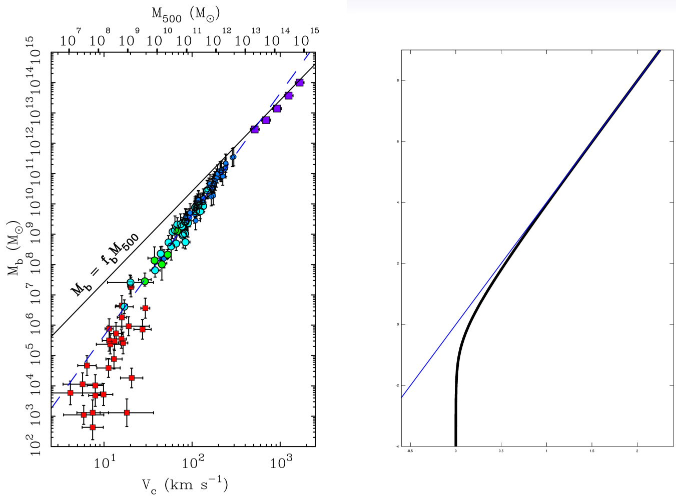

Figure : The curve on the right results from the wave dark matter theory if one assumes that, for two constants r_0 and ω_0, the time frequency of the wave dark matter a distance r_0 outside the galaxy is equal to ω_0.